Extracellular Matrix Metabolism in Bronchopulmonary Dysplasia: Focus on Lysyl Hydroxylases and Transglutaminases

Inauguraldissertation

zur Erlangung des Grades eines Doktors der Medizin

des Fachbereichs Medizin der

Justus-Liebig-Universität Gießen

vorgelegt von

Jörn Thilo Witsch

aus Freiburg

Gießen 2013

Aus dem Zentrum für Innere Medizin

Medizinische Klinik II und Poliklinik

Direktor: Prof. Dr. W. Seeger

Universitätsklinikum Gießen und Marburg GmbH, Standort Gießen

Gutachter: Prof. Dr. W. Seeger

Gutachter: Prof. Dr. M. Kracht

Tag der Disputation: 04.02.2013

Declaration

I declare that I have completed this dissertation single-handedly without the unauthorized help of a second party and only with the assistance acknowledged therein. I have appropriately acknowledged and referenced all text passages that are derived literally from or are based on the content of published or unpublished work of others, and all information that relates to verbal communications. I have abided by the principles of good scientific conduct laid down in the charter of the Justus Liebig University of Giessen in carrying out the investigations described in the dissertation.

Erklärung

Ich erkläre: Ich habe die vorgelegte Dissertation selbstständig ohne unerlaubte fremde Hilfe und nur mit den Hilfen angefertigt, die ich in der Dissertation angegeben habe. Alle Textstellen, die wörtlich oder sinngemäß aus veröffentlichten oder nicht veröffentlichten Schriften entnommen sind und alle Angaben, die auf mündlichen Auskünften beruhen, sind als solche kenntlich gemacht. Bei den von mir durchgeführten und in der Dissertation erwähnten Untersuchungen habe ich die Grundsätze guter wissenschaftlicher Praxis, wie sie in der "Satzung der Justus-Liebig-Universität Gießen zur Sicherung guter wissenschaftlicher Praxis" niedergelegt sind, eingehalten.

I. Contents

II. List of figures

III. List of abbreviations

ADAMTS	A disintegrin and metalloproteinase with thrombospondin motifs
APS	Ammonium persulfate
BMP	Bone morphogenetic protein
BPD	Brochopulmonary dysplasia / Bronchopulmonale Dysplasie
cDNA	Complementary DNA
cm	Centimeter
CMV	Cytomegalovirus
dH_2O	Distilled water
DNA	Deoxyribonucleic acid
ECM	Extracellular matrix
EDS	Ehlers-Danlos Syndrome
EDTA	Ethylendinitrilo-N, N, *N'*,*N'* -tetra-acetic-acid
Fig.	Figure
FGF	Fibroblast growth factor
h	Hour
HaCaT	Human keratinocyte cell-line
HRP	Horseradish peroxidase
Hspa8	Heat shock 70 kDa protein 8
IB	Immunoblot
IHC	Immunohistochemistry
IRDS	Infant respiratory distress syndrome
l	Liter
Lox	Lysyl oxidase
min	Minute
ml	Milliliter
mM	Millimolar

mRNA	Messenger RNA
NCPAP	Nasal continuous positive airway pressure
ng	Nanogram
NIH/3T3	Mouse embryonic fibroblast cell line
P1, 3, *etc.*	Postnatal day 1, 3, *etc.*
PAGE	Poly-acrylamide gel electrophoresis
paSMC	Primary human pulmonary artery smooth muscle cells
PBS	Phosphate-buffered saline
PCR	Polymerase chain reaction
Plod	Procollagen-lysine, 2-oxoglutarate 5-dioxygenase
PMA	Postmenstrual age
PPV	Positive pressure ventilation
rER	Rough endoplasmic reticulum
RNA	Ribonucleic acid
RT	Reverse transcriptase
SDS	Sodium dodecyl sulfate
TAE	Tris-acetate-EDTA
TEMED	*N, N, N',N'* tetramethyl-ethane-1,2-diamine
TGF	Transforming growth factor
Tgm	Transglutaminase
TNF	Tumor necrosis factor
u	Unit
UV	Ultraviolet
V	Volt
vol	Volume
Wk	Week
%	*Per cent*
®	Registered trademark
°C	Degree Celsius

Chapter 1

Introduction

1.1 Bronchopulmonary dysplasia

Bronchopulmonary dysplasia (BPD), also referred to as *neonatal chronic lung disease,* is a chronic pulmonary disorder of infants that are prematurely born with very low birth weight. Bronchopulmonary dysplasia is characterized by dysregulated lung development and may lead to a number of complications. Depending on the severity of the disease, complications include recurrent pulmonary infections[1], pulmonary hypertension[2], poor growth[3], impaired neurological development[4] and death. Bronchopulmonary dysplasia is the primary severe complication of preterm birth[5], having been first described in 1967 by W.H. Northway[6], and ever since has been noted to be a major cause of morbidity in neonatal intensive care units. Improved perinatal care has led to a shift in the histopathological presentation of the disease: the “classic” or “old” BPD that is characterized by extensive inflammatory changes in the lung is rarely seen today. It has been replaced by the milder “new” BPD that is characterized largely by decreased alveolar septation and an arrest of late lung development[7, 8].

Neonates born with infant respiratory distress syndrome (IRDS) are at increased risk for developing BPD. Severe cases of IRDS require endotracheal intubation with positive-pressure ventilation and high levels of supplemental oxygen in order to maintain an acceptable blood oxygen-saturation. These supportive procedures lead to lung injury resulting in BPD[9]. Further risk factors include congenital heart disease[10], antenatal infections, like chorioamnionitis[11], and postnatal respiratory infections with CMV and *Ureaplasma*[12].

1.1.1 Clinical presentation and diagnosis

The clinical symptoms of BPD are relatively non-specific and consist of cyanosis, chronic cough, rapid breathing and shortness of breath. Helpful measures that

support the diagnosis of BPD include blood-oxygen levels, which may reveal hypoxemia and hypercarbia; and chest imaging[13], which may demonstrate emphysema as well as atelectasis. Bronchopulmonary dysplasia is typically suspected when a ventilated neonate can not be weaned from the supportive O_2-therapy. According to a National Heart, Lung and Blood Institute workshop in 2001[2], diagnostic criteria include oxygen-requirement of infants at a certain postnatal day. Bronchopulmonary dysplasia is subdivided into mild, moderate and severe BPD depending on the amount of oxygen required and on the gestational age of the newborn (Table 1).

Table 1. Diagnostic criteria* and categorization of the severity of BPD (Modified from Jobe *et al*. 2001).

<32 wk Gestational age†	≥32 wk Gestational age‡	Diagnosis
Breathing room air at 36 wk PMA or discharge, whichever comes first	Breathing room air by 56 days postnatal age or discharge, whichever comes first	Mild BPD
Need for <30% O_2 at 36 wk PMA or discharge, whichever comes first	Need for <30% O_2 at 56 days postnatal age or discharge, whichever comes first	Moderate BPD
Need for ≥30% O_2, positive pressure, or both at 35 wk PMA or discharge, whichever comes first	Need for ≥30% O_2, positive pressure, or both at 56 days postnatal age or discharge, whichever comes first	Severe BPD

*These criteria are in addition to the baseline requirement of >21% O_2 for at least 28 days.
†Assessed at 36 wk postmenstrual age (PMA).
‡Assessed at age 29 to 55 days.

PMA = Post menstrual age, wk = Weeks.

However, there are no accepted standards for supplemental oxygen administration which sets limitations on the use of supplemental oxygen as a criterion for BPD diagnosis. In order to overcome this problem, a physiological definition of BPD was established[14]. According to this definition, at 36 ± 1 weeks PMA, infants treated with positive pressure support, or supplemental oxygen concentrations of >30% and

oxygen saturations of 90-96% were diagnosed with BPD without additional testing. Infants receiving ≤30% oxygen or oxygen >30% with saturations >96% underwent a timed, stepwise reduction to room air with continuous observation and oxygen-saturation monitoring. "No BPD" was defined by oxygen-saturations ≥90% under room air for 30 minutes. "BPD" was defined by oxygen-saturations <90%. This new definition led to a reduction of the overall rate of BPD, and reduced the variation in the rate of BPD among centers.

1.1.2 Epidemiology

Owing to improved prenatal care in high risk patients, the clinical and pathological features of BPD have changed in recent years. Moreover, diagnostic criteria used to define BPD have been changing constantly with the changing nature of the disease. This complicates the monitoring of the incidence of BPD. Clearly the incidence of BPD decreases with advanced gestational age of the neonates. The disease rarely occurs beyond 32 weeks gestational age[15].

A study from 2001[16] reports an oxygen-dependence of 23% at 36 weeks among infants with a birth weight less than 1500 g. In 2003, another study[17] demonstrated an oxygen-dependence of 53.2% at 36 weeks among infants born before 28 weeks gestational age. This points out that improved medical care does not, as one might expect, lead to a decrease in the incidence of BPD. Conversely, the use of antenatal glucocorticoids, postnatal surfactant treatment, and advanced respiratory and nutritional support in modern medicine may even lead to an increase in BPD incidence. Even the smallest premature infants now have a chance of survival due to these supportive measures. Yet, these infants are highly susceptible to lung damage through high pressure mechanical ventilation and oxygen toxicity maintaining a high, or possibly even increasing the incidence of BPD.

1.1.3 Lung development and the pathogenesis of BPD

Lung development is a lengthy process starting around the third week of the embryonic period and is completed in childhood at approximately 2-3 years of age, when the adult number of alveoli is reached. However, the size and surface area may increase until after adolescence[18]. At the end of the canalicular stage, between weeks 16 and 24 (Fig. 1), independent respiration is possible, however, survival rates of infants born at this stage of lung development are low. In the following saccular

stage, between week 24 and birth, the airspaces expand and surfactant is produced by pneumocytes. During this period, newborns have a much higher chance of survival. However, due to still markedly underdeveloped lungs early in this period, respiratory support of the newborns is often necessary. Positive pressure ventilation with oxygen-rich gas can cause chronic injury to the developing lung and is a major risk factor in the pathogenesis of BPD[19]. The ventilation disrupts critical signaling pathways, which results in failed formation of the alveoli[20] and the pulmonary vasculature[21, 22, 23], a decrease in alveolarization and, hence, a smaller gas-exchange surface in the lung.

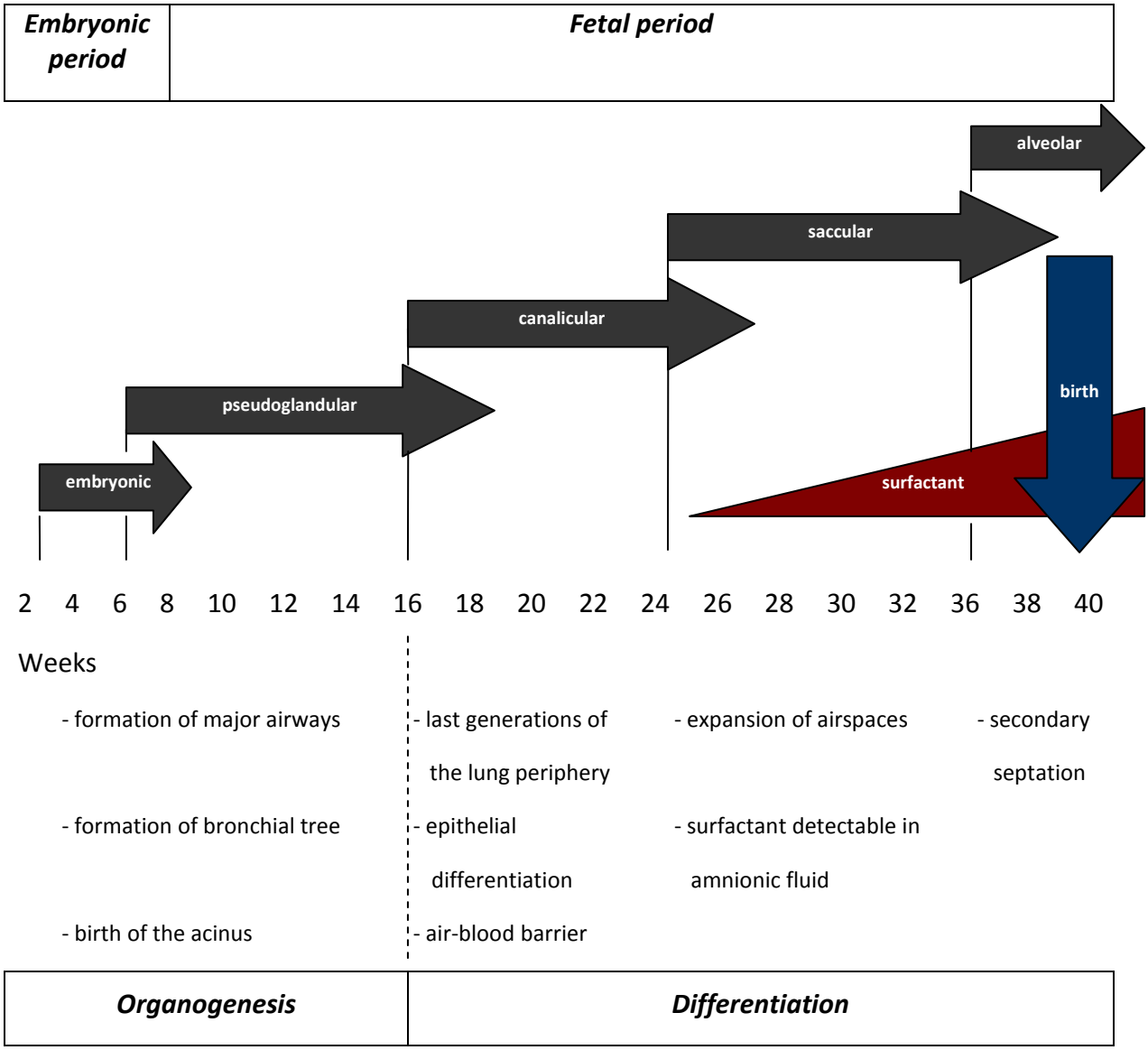

Figure 1. The stages of human lung development and their features (modified from www.embryology.ch).

Extensive research has been invested to understand the mechanism of how oxygen might contribute to chronic inflammation and injury in the neonatal lungs. For example, in a mouse model of chronic exposure to hyperoxia, high oxygen supplementation (85%) led to a detectable increase in the expression of pro-inflammatory cytokines and a decrease in cell proliferation[24].

However, understanding of the pathomechanisms underlying the pronounced arrest of alveolar septation is incomplete. To date, there are several publications that hint at a key role of lung extracellular matrix (ECM) metabolism in the development of BPD. Specifically, an incompletely understood dysregulation of collagen-[25] and elastin metabolism[26,27] leads to a disturbed pulmonary ECM architecture.

1.2 Extracellular matrix and the developing lung

The ECM, by definition being any material part of a tissue that is not part of a cell, is the defining feature of connective tissue. The ECM consists of glycoproteins such as collagen (the most abundant ECM protein in animals), fibrin, elastin, fibronectin and laminin. Moreover, the ECM contains minerals such as hydroxyapatite, and water. The ECM functions mainly as a support and anchorage substrate for cells, as a local depot for a wide range of growth factors, as a regulator of intercellular communication and separates different tissues from each other.

The ECM controls cellular growth, migration and differentiation in the developing lung. In turn, a variety of peptides, cytokines and growth factors, which are secreted from pulmonary cells, regulate gene expression, RNA processing and the translation of pulmonary ECM proteins[28]. The ECM proteins are crucial for proper branching of airways and alveolarization in the developing lung[29]. The ECM constituents are discharged from the cell for anchoring or communication, or serve as membrane receptors. The metabolism of ECM proteins, possibly including posttranslational modifications, is affected by changes in the cellular biochemical environment, such as changes in oxygen concentration[30].

Normal lung development follows a genetically programmed pattern and is dependent on the undisturbed interaction between cells and the ECM. During late lung development, primarily in the postnatal period, the lung gas exchange surface is expanded. This branching of airways is, in part, directed by the interaction of the epithelium with the underlying splanchnic mesoderm. Growth factors such as

fibroblast growth factor (FGF)[31], transforming growth factor (TGF)-β[32] and bone morphogenetic protein (BMP)[33] are implicated in the growth and differentiation of the lung airway epithelium into the multiple cell lineages required for postnatal respiratory tract formation. These growth factors are engaged in multiple pathways that act individually and as a network. Minor disruptions to this process may affect the immature lung, leading to a pronounced decrease in lung function.
A better understanding of the intercellular communication, the intracellular signaling pathways and extracellular metabolic pathways is essential to gain insight into the pathomechanisms of BPD.

1.3 Collagen processing in ECM assembly

Collagen synthesis starts at the gene level. Each collagen type has a unique primary sequence and, therefore, a specific mRNA. After mRNA processing, the translation, as with most other proteins that are destined for the ECM, takes place at the rough endoplasmatic reticulum (rER). The translation product, the preprocollagen (also called α-chains), contain a signal peptide, and is translocated into the lumen of the rER. Preprocollagen has an unusual sequence: approximately every third amino acid is glycine and about 17% of all amino acid residues are proline residues. Relative to the location of glycine emerges another important amino acid: lysine. Inside the rER lumen, proline and lysine residues undergo hydroxylation by prolyl hydroxylases or lysyl hydroxylases, respectively (Fig. 2). These reactions are vitamin C-dependent and represent a very important step in the posttranslational modification of collagen. Insufficient hydroxylation may lead to defective collagen molecules and damage ECM formation. Hydroxylysine residues are then glycosylated, where the triple helical structure can be formed. Alternatively the residues serve as anchorage points for covalent cross-links between the collagen molecules (this cross-link also occurs in other proteins with *collagen-like* domains)[34]. Hydroxyproline stabilizes the triple helix by forming hydrogen-bonds between the chains. After the so-called “procollagen” is secreted from the cell, the extension peptides from the *termini* of the molecule are removed by the metalloproteinases ADAMTS-2 (A disintegrin and metalloproteinase with thrombospondin motifs-2) and bone morphogenetic protein (BMP)-1. The cleaved extension peptides, in turn, are believed to reenter the cell and regulate

collagen synthesis via a feed-back mechanism[35]. Finally, the molecule resides in the extracellular space and is now called collagen. To form collagen fibrils and fibers which provide extraordinary strength to the mature collagen structures, a reaction catalyzed by lysyl oxidase is required[36]. Lysyl oxidase forms inter- and intra-cellular cross links within or between collagen fibers, which represents the most critical posttranslational modification. The ready-made collagen fibers can now establish, together with other proteins including elastin and fibronectin, the ECM.

The fibers of the ECM, however, do not present a rigid structure. As described below, in Chapter 1.5, other enzymes, including transglutaminases, may enhance the number of cross links between proteins in the extracellular space, in order to further stabilize the ECM.

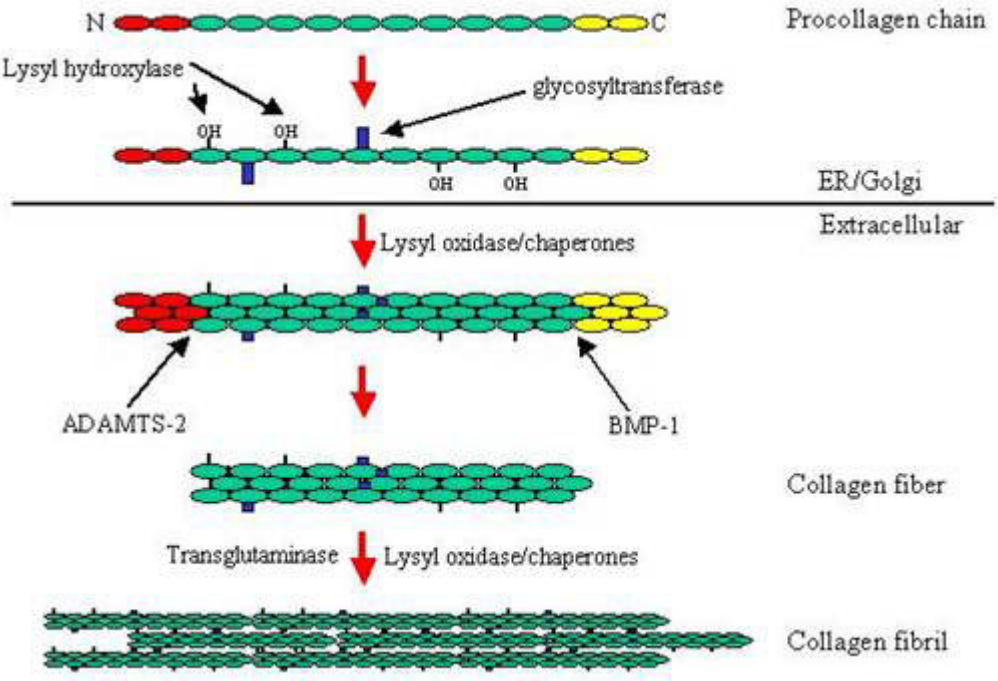

Figure 2. The intra- and extracellular steps of collagen synthesis.

ER = Endoplasmic reticulum, ADAMTS = A disintegrin and metalloproteinase with thrombospondin motifs, BMP = Bone morphogenetic protein

1.4 ECM remodeling and TGF-β signaling

Several studies have investigated disturbed structural synthesis and production of ECM proteins in BPD. For example Thibeault *et al.*[37] described an increase in interstitial collagen deposition caused by prolonged mechanical ventilation of premature infants. These collagen fibers, apart from an increase in quantity, were characterized as being "*disorganized, tortuous, and thickened*" (Fig. 3).

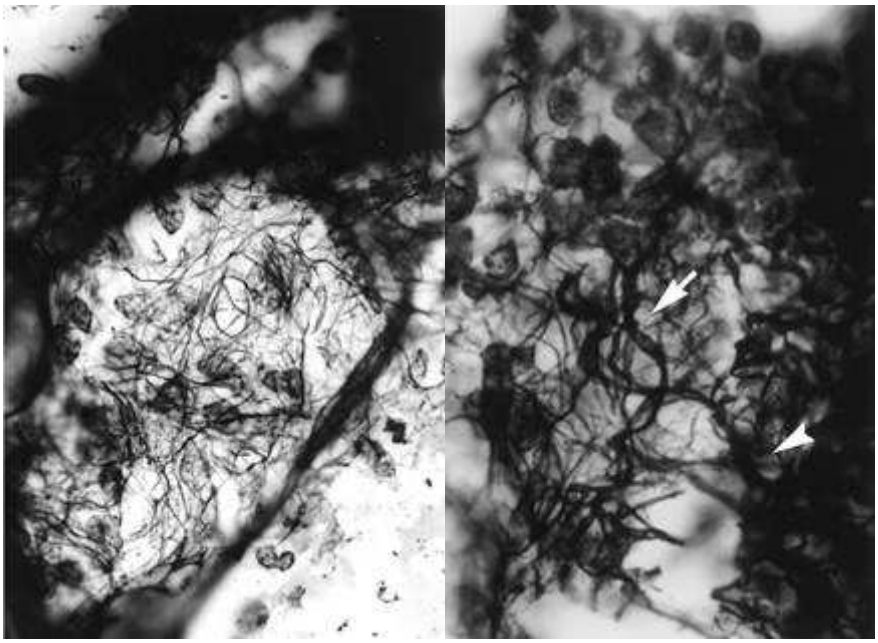

Figure 3. *En face* sections through alveolar septal walls of two premature infants (taken from Thibeault *et al.*[37]).
Left, *S*ection of a 30-week-gestation control lung. There is a continuous mesh of fine and coarse collagen fibers connecting to the large fibers at the air sac mouth.
Right, Section of a 24.4-week gestational age infant that died at 28.8 weeks post conception. The arrow points out a thickened, tortuous secondary fiber. The arrowhead points out secondary fibers uniting with a thick tertiary fiber.

However, relatively few studies have addressed posttranslational modifications, stabilization and breakdown of ECM proteins. A connection between the pathogenesis of BPD and enhanced ECM cross-linking has already been suggested by Pierce *et al*.[26] in 1997. In this study, an increase in desmosine, a marker of cross-linked elastin, as well as an increase in elastin production, was observed in the lungs of mechanically ventilated preterm lambs. In 2009, the expression of lysyl

oxidase, an enzyme important for ECM protein cross-linking, was found to be up-regulated in mice after exposure to a hyperoxic gas mixture. Likewise, up-regulation of lysyl oxidase expression was found in the lungs of infants that died with BPD or were at risk of developing BPD[38]. It was hypothesized that this might result in an "over-stabilization" of collagen and elastin molecules and, hence, of the ECM. Because TGF-β is believed to be a highly important growth factor in late lung development[39] and in the pathogenesis of BPD[40,41], the effect of TGF-β on lox gene (encoding lysyl oxidase) expression was examined in this study. Enhancement of lox gene expression in the developing mouse lung was observed to be partly driven by abnormal TGF-β signaling. As early as in 2006[42] hyperoxia was shown to potentiate TGF-β signaling in lung fibroblasts which, in turn, enhanced the production of a number of ECM proteins, including the α_1-subunit of type I collagen, tissue inhibitor of metalloproteinase-1, tropoelastin, and tenascin-C.

Given these data and the variety of enzymes responsible for ECM remodeling, it is highly promising to look at other types and families of ECM cross-linking enzymes: therefore, in the present study, lysyl hydroxylase and transglutaminase expression was examined with respect to TGF-β stimulation, and the impact of normobaric hyperoxia in an animal model.

1.5 ECM cross-linking enzymes

1.5.1 Lysyl Hydroxylases

Lysyl hydroxylases are enzymes that catalyze the vitamin C-dependent hydroxylation of lysine residues in collagen and collagen-like proteins, resulting in the formation of a hydroxylysine residue (Fig. 4).

This occurs inside the rER prior to triple-helix formation. These hydroxylated lysine residues are later either glycosylated or required for the formation of covalent and irreversible cross-links between collagenous molecules and, hence, are crucial for the maturation of the ECM.

The lysyl hydroxylases, which are also referred to as procollagen-lysine, 2-oxoglutarate 5-dioxygenase (Plod) enzymes, occur as three different enzymes, encoded by three different genes in human, rat and mouse tissue: Plod1, Plod2 and Plod3.

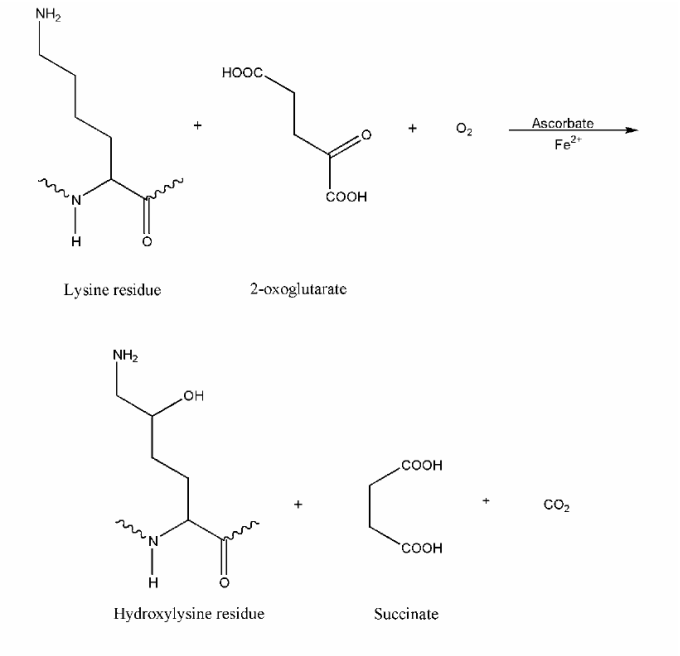

Figure 4. Hydroxylation reaction of a lysine residue in a collagenous sequence catalyzed by lysyl hydroxylase. One oxygen molecule is needed to hydroxylate the lysine residue and to decarboxylate 2-oxoglutarate. The CO_2 is liberated by this reaction (taken from Puistola *et al.*)[43].

The Plod1 gene product, the lysyl hydroxylase 1, is responsible for lysyl hydroxylation in the helical part of collagen type I. Mutations in the PLOD1 gene lead to a heritable disorder of the connective tissue, characterized by joint hypermobility and skin fragility and hyperextensibility: *the Ehlers-Danlos Syndrome Type VI (EDS VI)*[44].

Plod2 exists in two alternatively-spliced forms. The shorter isoform (Plod2a) is, so far, only known to be expressed in the human kidney, spleen, liver and placenta. Plod2b, the longer isoform, demonstrated its significance in ECM disorders in a study from 2004[45], where increased formation of pyridinoline cross-links was found to be a consequence of increased expression of Plod2b. The pyridinoline cross-link is the product of a lysyl-oxidase catalyzed reaction and is elevated in a variety of fibrotic disorders including systemic scleroderma. Also, Plod2 exhibits an increased transcriptional activity in systemic sclerosis[46], which suggests a possible connection between elevated levels of Plod2, increased pyridinoline cross-linking and fibrotic tissue formation.

A mutation in the Plod2 gene results in Bruck's syndrome, a recessively inherited ECM disorder characterized by skeletal changes similar to *osteogenesis imperfecta* and contractures of the large joints[47].

The third member, Plod3, in addition to playing a role in lysyl hydroxylation, possesses glucosyltransferase and galactosyltransferase activities[48]. Moreover, Plod3 has an important role in the dynamic remodeling of the ECM[49], as Plod3 is localized both intra- and extra-cellularly. In the extracellular space, Plod3 can adjust the amount of hydroxylysine and hydroxylysine-linked carbohydrates of extracellular proteins[50]. In Plod3 knockout mice, collagen IV synthesis is impaired, which results in disturbed basement membrane formation and, thus, abnormal embryonic development and embryonic death[51].

All Plod genes have been described to be widely expressed during mouse embryogenesis (Plod1 being the most highly expressed) with similar expression patterns and tissue location[52]. In adult cells, the Plod distribution profiles become more specialized. The Plod1 and Plod2 members are mainly localized inside the rER lumen, whereas Plod3, depending on the tissue-type, can be present inside as well as outside the cell. However, in lung tissue, where all three isoforms are highly expressed, Plods were, by light microscopy, localized only intracellularly and expression was very cell specific: Plod2 in smooth muscle bundles of the bronchioles, and Plod3 in type II pneumocytes[53].

Based on a study by Alejandre-Alcázar *et al*.[42] that demonstrated that hyperoxia induced TGF-β, and TGF-β, in turn, up-regulated several ECM proteins, one could hypothesize that TGF-β might also induce Plod genes. Yet, there is little information available in the literature about the possible influence of TGF-β on lysyl hydroxylase expression. In human osteoblasts, lysyl hydroxylation in collagen, particularly in the collagen α_2 chain, was decreased by TGF-β1. Moreover lysyl hydroxylase mRNA levels were reduced, whereas mRNAs for collagen α-chains were stimulated by TGF-β[54]. Similar tendencies were observed in adipose tissue-derived mesenchymal stem cells, where TGF-β1 down-regulated the expression of Plod3[55]. However, in 2005, a study found that several cytokines, including all three isoforms of TGF-β, influenced the collagen cross-linking pathway by up-regulating Plod2b mRNA levels as well as the abundance of the pyridinoline cross-link, which is increased in several fibrotic disorders[56]. This up-regulation of Plod2b expression, observed in skin fibroblasts, was higher, even relatively to the up-regulation of the expression of the collagen α_2 chain, suggesting more cross-links per collagen molecule.

1.5.2 Transglutaminases

The transglutaminase (Tgm) family of enzymes is a ubiquitously expressed group of intra- and extra-cellular enzymes that catalyze a calcium-dependent posttranslational modification reaction: the transamidation of glutamine residues (Fig. 5).

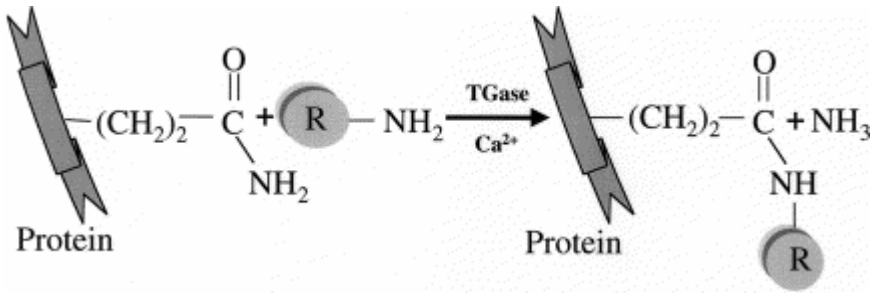

Figure 5. The transglutaminase-catalyzed reaction between the γ-carboxamide group of a peptide-bound glutamine and the primary amine group of a peptide-bound lysine. The product is the γ-glutamyl-ε-lysine cross-link, levels of which are increased in many fibrotic disorders (taken from Chen *et al*.[57]).

This results in the formation of γ-glutamyl-ε-lysine cross-links, which are highly resistant to proteolysis, and stabilize the ECM proteins in a variety of tissues against chemical, enzymatic or mechanical breakdown.

There are nine different tranglutaminase-genes[58] that have been identified in mammals (Table 2). Yet, only eight of these genes encode active enzymes.

Transglutaminase-mediated cross-linking is believed to be involved in the pathogenesis of a variety of diseases such as lamellar ichthyosis, psoriasis (for Tgm1) Alzheimer's disease, Parkinson's disease, Huntington's disease and cardiovascular diseases[59,60] (for Tgm2).

Transglutaminase 1, although also called keratinocyte transglutaminase, has also been described to be expressed in lung tissue, more specifically in normal bronchial epithelium[61]. The role of Tgm1 has been extensively studied in the epidermis where it is involved in the maintenance of skin tissue integrity and impermeability as well as in cell envelope formation in the differentiation of keratinocytes[62]. Transglutaminase 1 activity in keratinocytes is primarily membrane-bound[63]. The Tgm1 is believed to be a marker for squamous differentiation and to be useful in evaluating the degree of differentiation in benign and malignant oral epithelial proliferation[64]. However, little is

known about Tgm1 function in the lung, making it an interesting target for investigation in the context of ECM remodeling disturbances in BPD.

Table 2. The mammalian transglutaminase family and its distribution in tissues and cell-components. (Modified from Esposito *et al*.[65]).

Name	Synonyms	Tissue	Location
Tgm1	Keratinocyte Tgm, TG_K	Epithelia	Cytosolic, membrane
Tgm2	Tissue Tgm, TG_C	Ubiquitous	Cytosolic, nuclear, extracellular
Tgm3	Epidermal Tgm, TG_E	Epithelia	Cytosolic
Tgm4	Prostate Tgm, TG_P	Prostate	Extracellular
Tgm5	TG_X	Epithelia	Cytosolic
Tgm6	TG_Y	Unknown	Unknown
Tgm7	TG_Z	Ubiquitous	Unknown
FXIII	Factor XIIIA, fibrin stabilizing factor	Blood plasma, platelets	Extracellular
Band 4.2	Erythrocyte protein band 4.2	Erythrocytes	Membrane

Transglutaminase 2, in contrast, is an enzyme that is expressed in a large variety of tissues and occurs in an intracellular as well as in an extracellular form and, hence, post-translationally modifies intra- and extra-cellular proteins. The Tgm2 is involved in cell death and differentiation, matrix stabilization and serves as an adhesion protein. The extracellular Tgm2 is secreted, usually in very small amounts, from the cell into the extracellular space, where it is implicated in the cell-ECM interactions by cross-linking matrix proteins[66]. Many proteins that are needed for stabilization and remodeling of the ECM, such as collagen, fibronectin, fibrinogen/fibrin, vitronectin, osteopontin, laminin and nidogen, have been identified as substrates of Tgm2[62]. Stress on a cell often leads to an up-regulation of Tgm2 and further secretion of the enzyme into the matrix. Furthermore, intracellular Tgm2 leaks from dying cells into the extra cellular space, resulting in massive matrix cross-linking and scar tissue formation. Tgm2 expression and, thus, the abundance of the γ-glutamyl-ε-lysine

crosslink, are enhanced in all fibrotic disorders that are characterized by excessive scar tissue formation, including lung fibrosis[67, 68].

Transglutaminase 2 is further presumed to be involved in chronic inflammatory diseases by enhancement of TGF-β activation in the ECM[69, 70]. Elevated levels of TGF-β can lead to increased matrix deposition and, additionally, have been described to up-regulate pulmonary TGM2 expression[71], both possibly resulting in over-stabilization of the ECM. These findings suggest a complex, mutual control mechanism between Tgm2 and TGF- β.

Another interesting feature of Tgm2 was observed during lung development. In newborn rats, Tgm2 enzyme activity was detected before term, whereas the γ-glutamyl-ε-lysine crosslink was detected for the first time between postnatal days 10 and 19[72]. In the larger airways and vessels of the lung, where maturation is known to occur earlier, the γ-glutamyl-ε-lysine cross-link as well as the extracellular Tgm2 appeared at the end of the first postnatal week. It was concluded that Tgm2 presence and activity could be used as a marker for postnatal lung maturation. The irreversible crosslinking is believed to be enhanced towards the end of lung-development in order to stabilize the final structure of the organ. Irregularities in the expression of Tgm2, like premature enzyme upregulation, may therefore result in over-stabilization and impaired remodeling of the ECM and early termination of lung organogenesis.

Chapter 2

Hypothesis and Aims

Bronchopulmonary dysplasia is a dangerous complication of prematurity. Although several causes and risk factors for BPD have been identified, exact knowledge about the pathogenesis of BPD is still lacking. Many publications assume disturbances in pulmonary ECM metabolism as one of the causes that lead to impaired lung development and respiratory function. This is thought to be caused by abnormal cytokine signaling. Dysregulation of ECM cross-linking enzymes as well as TGF-β signaling has been demonstrated by several studies. However, little is known about which cross-linking enzymes are abnormally active or expressed in BPD. In this context, the expression of lysyl hydroxylases and tranglutaminases was examined using a chronic hyperoxia mouse model of BPD. Moreover, signaling pathways that possibly regulate these cross-linking enzymes are poorly investigated. Here, the effect of TGF-β and hyperoxia on the expression of lysyl hydroxylases and tranglutaminases in different cell lines was studied.

2.1 Hypothesis

Based on the rationale outlined above, it was hypothesized, that

- The expression of lysyl hydroxylases and transglutaminases is altered during pathological late lung development.
- Dysregulation of lysyl hydroxylases and transglutaminases is triggered by hyperoxia and/or the growth factor TGF-β.

2.2 Aims

Hence, the aims of the study were

- To determine whether the expression of lysyl hydroxylases and transglutaminases change in a mouse model of BPD.
- To investigate whether the expression of lysyl hydroxylases and transglutaminases is influenced by hyperoxia and/or TGF-β.

Chapter 3

Materials and Methods

3.1 Materials

3.1.1 Technical equipment and manufacturer

Equipment	*Manufacturer*
Developing machine; X Omat 2000	Kodak, USA
Electrophoresis chambers	Bio-Rad, USA
Film cassette	Sigma-Aldrich, Germany
Filter Tip FT: 10, 20, 100, 200, 1000	Greiner Bio-One, Germany
Freezer -20 °C	Bosch, Germany
Freezer -40 °C	Kryotec, Germany
Freezer -80 °C	Heraeus, Germany
Fridge +4 °C	Bosch, Germany
Gel blotting paper 70 x 100 mm	Bioscience, Germany
Glass bottles: 250, 500, 1000 ml	Fisher, Germany
Mini spin centrifuge	Eppendorf, Germany
Multifuge centrifuge, 3 s-R	Heraeus, Germany
Nanodrop ®	Peqlab, Germany
PCR-thermocycler	MJ Research, USA
PCR-tubes (0.2 ml)	Applied Biosystems, USA
Pipetboy	Eppendorf, Germany
Pipetmans: P10, P20, P100, P200, P1000	Gilson, France
Quantity One software	Bio-Rad, Germany
Radiographic film X-Omat LS	Sigma- Aldrich, Germany
Serological pipette: 5, 10, 25, 50 ml	Falcon, USA
Single-use syringe	Braun, Germany

Test tubes: 15, 50 ml	BD Biosciences, USA
Trans blot transfer membrane (0.2 µm)	Bio-Rad, USA
Vortex machine	Eppendorf, Germany
Vacuum centrifuge	Eppendorf, Germany
Western blot chambers:	
Mini Trans-Blot	Bio-Rad, USA
Mini-Protean 3 Cell	Bio-Rad, USA

3.1.2 Reagents and source of supply

Reagents	*Source of supply*
Acetone	Roth, Germany
Acrylamide solution, Rotiphorese Gel 30	Roth, Germany
Agarose	Invitrogen, UK
β-mercaptoethanol	Sigma-Aldrich, Germany
Bromophenol blue	Sigma-Aldrich, Germany
DNA Ladder (1 kb)	Promega, USA
Dulbecco´s phosphate buffered saline 10×	PAA Laboratories, Austria
Dulbecco´s phosphate buffered saline 1×	PAA Laboratories, Austria
Ethylendinitrilo-N, N, *N',N'*-tetra-acetic-acid (EDTA)	Promega, USA
Ethanol absolute	Riedel-de Haën, Germany
ECL Plus Western Blotting Detection System	Amersham Bioscience, UK
Ethidium bromide	Roth, Germany
Gel extraction kit	Qiagen, Germany
Glycine	Roth, Germany
Magnesium sulfate	Sigma-Aldrich, Germany
Methanol	Fluka, Germany
N,N,N',N'-tetramethyl-ethane-1,2-diamine (TEMED)	Bio-Rad, USA
Oligo$(dT)_{15}$ primer	Promega, USA
PCR Nucleotide Mix	Promega, USA

2-Propanol	Merck, Germany
QIAprep Spin Miniprep Kit	Qiagen, Germany
Quick Start™ Bradford Dye Reagent	Bio-Rad, USA
RNAsin inhibitor	Promega, Germany
RNeasy Midi Kit	Qiagen, Germany
Smooth muscle cell medium 2	Promocell, Germany
SuperSignal® West Pico Chemiluminescent Substrate	Pierce, USA
Tris	Roth, Germany
Trypsin/EDTA	Gibco BRL, Germany
Tween 20	Sigma-Aldrich, Germany

3.2 Methods

3.2.1 Animal and tissue treatment

All animal procedures were approved by the animal ethics authority of the government of the state of Hessen (Regierungspräsidium Giessen II25.3–19c20 – 15(1) GI20/10-Nr.22/2000).

A mouse model of chronic exposure to hyperoxia

Mice are excellent animals to study pulmonary diseases of prematurity. Mouse pups are born in the saccular stage of lung development, which mimics the pulmonary conditions in premature human infants that are born between the 24th and 36th week of gestational age.

Newborn - as well as adult - C57BL/6J mice were maintained in humidity- and temperature-controlled rooms. Mice were allowed food and water *ad libitum* and were maintained on a 12h-12h light-dark cycle. Neonates from four to eight litters, which were born within a maximum of three hours apart, were pooled on their first day of birth (P1). After randomizing pups to nursing dams, these pups were separated into two equally sized groups: 50% remained in room air [21% (vol/vol) O_2], while the other 50% were maintained in 85% O_2. In order to prevent oxygen toxicity to the nursing dams, dams were exchanged between hyperoxic and normoxic conditions every 24 h. Pups were housed in 90 × 42 × 38 cm Plexiglas chambers that were

ventilated continuously at a flow rate of 3.5 l/min. A Miniox II monitor (Catalyst Research, Owing Mills, MD) was used to control oxygen concentration inside the chambers at all times. To measure dynamic compliance, the volume-pressure compliance method in anesthetized mice, as described previously[73], was utilized. At postnatal days 1, 7, 14, 21 and 28 mice were killed for analysis. These four weeks after birth span the period of late lung development in mice.

Processing of lung tissue

Mice were killed by an intraperitoneal injection of sodium pentobarbital. After opening the aorta, mice bled out and the heart and lungs could be excised *en bloc*. The lungs were pressure-fixed overnight at 20 cmH_2O with 4% (mass/vol) paraformaldehyde in phosphate-buffered saline (PBS; 20 mM Tris-Cl, 137 mM NaCl, pH 7.6), and then cut into 3-µm sections and mounted on glass slides.

3.2.2 Human tissue

The Human Subjects Review Committees of the Erasmus University Medical Centre and the University of Giessen Lung Center approved the utilization of human material. The neonatal lung tissue used in this work accrued from archived autopsy material at the Erasmus University Medical Centre and the University of Giessen Lung Center.

3.2.3 Cell culture

Mouse NIH/3T3 fibroblast-like cells (American Type Culture Collection), primary human pulmonary artery smooth muscle cells (paSMC) (Promocell) and cells from the human keratinocyte cell-line (HaCaT) (Lonza) were cultured and assessed for dysregulation of ECM enzyme expression under hyperoxic condition and/or TGF-β stimulation. The cells were maintained under 21% O_2 or 85% O_2 for 24 h, prior to stimulation with TGF-β1 (2 ng/ml) for a further 24 h. Gas tension in the culture media was monitored daily.

3.2.4 RNA isolation

The RNA derived from the cell cultures and isolation was accomplished following the manufacturer's instructions provided with the RNeasy Midi Kit.

3.2.5 Assessment of RNA concentration

For assessment of the concentration and quality of the RNA isolated from the cell lines, 1.5 µl from the sample RNA was inserted into a Nanodrop® spectrophotometer. Absorbance was measured at 260 nm.

3.2.6 Reverse transcription reaction

The reverse transcriptase polymerase chain reaction, abbreviated as RT-PCR, is a technique where a RNA strand is reverse transcribed into its complementary DNA (cDNA) (in the RT step) and then amplified using the PCR. The RT-step is catalyzed by the enzyme *reverse trancriptase (RT)*. The PCR is catalyzed by DNA polymerase. In this reaction, cDNA is synthesized using a single strand of RNA as a template.

The RT reaction was performed using the *Improm-II Reverse Transcriptase* kit purchased from Promega (USA).

The RT reaction was carried out by assembling a mixture composed of 500 ng of RNA from the experimental lungs and 4 µl of oligo$(dT)_{15}$ (100 µg/ml) to prime the reaction. This was diluted with RNAse-free water to 10 µl final volume. This mixture was heated in a thick-walled PCR tube, at 70 °C for 5 min. This process denatures the double-stranded RNA into single strands and, hence, provides access for the primers to bind precisely to the polyA tail of the mRNA strand. Immediately after, the PCR tube was chilled on an ice medium for at least 5 min. Thereafter the RT-Mix (Table 3) reaction components were added.

Table 3: Components of the RT-Mix (Promega).

Reaction components	**Volume** (µl)	**Final concentration**
ImProm-II™ 5× Reaction Buffer	4.0	1×
$MgCl_2$ (25 mM)	4.8	6 mM
dNTP Mix (10 mM)	1.0	0.5 mM
RNasin® Ribonuclease Inhib. ImProm-II™	1.0	1 unit
Reverse transcriptase	1.0	1 unit
RNAse free water	3.2	Not applicable
Total Volume	15.0	**-**

After the reaction components were mixed by pipetting, the tubes were placed in the PCR machine, where the RT-PCR program was carried out. This program consists of three steps: the first step causes the *linearization of the RNA*. For this purpose the mix was warmed up to 25 °C for 5 min. For the next step, the *cDNA synthesis*, the tube was heated to 42 °C. During the third and last step, the sample was cooled down to 4 °C. This so-called *chilling* was carried out over night.

For cDNA synthesis from the mRNA isolated from cell-cultures, the *Sensiscript® Reverse Transcriptase Kit* from Qiagen, which can reverse-transcribe less mRNA, was used. The step of RNA denaturation in RNAse free water was performed at 65 °C for 5 min. Again the samples were chilled on ice and then mixed with the RT-Mix as described in Table 4.
The cDNA produced by these reactions was either used immediately for amplification via PCR or was stored in a freezer at -20 °C for later use.

Table 4. The Sensiscript RT-Mix (Qiagen).

Reaction Components	**Volume** (µl)	**Final Concentration**
10× Buffer RT	2.0	1×
dNTP Mix (5 mM each dNTP)	2.0	0.5 mM each dNTP
Oligo-dT primer (10 µM)	2.0	1 µM
RNAse inhibitor (10 u/µl)	1.0	10 u (per reaction)
Sensiscript Reverse Transcriptase	1.0	
RNAse-free water	Variable	not applicable
Template RNA	Variable	<50 ng (per reaction)
Total volume	**20.0**	-

3.2.7 Semi quantitative polymerase chain reaction

The polymerase chain reaction (PCR) is an enzymatic reaction used to amplify strands of DNA, in this case cDNA, which were generated from mRNA in the RT reaction. The PCR reaction was used to assess gene expression by exponentially amplifying the DNA sequence of interest. The enzyme used for this reaction is a special heat-resistant DNA polymerase, the Taq polymerase. Each PCR-reaction consists of three steps.

1. *Denaturation*: The double stranded DNA in the sample is being denatured by heat. Hydrogen bonds are broken, which results in single stranded DNA molecules.
2. *Annealing:* The primers in the sample bind to the appropriate sites on the single-stranded DNA.
3. *Elongation:* The Taq polymerase synthesizes a new DNA strand complementary to the template.

Each reaction, or cycle, doubles the amount of DNA in the sample. Thus, DNA strands multiply exponentially with the cycle number of the PCR reaction.

3.2.7.1.1 Semi quantitative PCR protocol

The polymerase used in this reaction was *GoTaq®Flexi DNA Polymerase* from Promega, in a final volume 25 µl. Apart from the DNA and the polymerase, a PCR mix with the components (listed in Table 5) was prepared.
An example of thermal cycling conditions for PCR amplification is presented in Table 6; however, the annealing temperature may vary with different primers (the primers used in the PCR reaction and the different annealing temperatures are listed in Table 7).

Table 5. Semiquantitative PCR mix

Components	**Volume** (µl)	**Final concentration**
5x Green GoTaq Flexi Buffer	5.00	1x
$MgCl_2$ solution (25 mM)	2.00	2 mM
PCR Nucleotide Mix (10 mM)	0.50	0.2 mM each dNTP
Upstream primer	0.50	0.2 µM
Downstream primer	0.50	0.2 µM
GoTaq Polymerase (5 u/µl)	0.25	1.25 u (per reaction)
Template DNA	~1-2 µl	<0.25 µg/25 µl
Nuclease-free water up to	25.00	-
Total Volume	~35	-

Again the components were combined and mixed by pipetting, before placing the tubes in the PCR machine.

The three crucial steps *denaturation, annealing and elongation (extension)* are repeated, depending how many copies are needed. Each cycle means a doubling of the amount of DNA that was in the tube at the beginning of the new cycle. This means an exponential increase of DNA in the sample with the number of cycles.

Table 6. PCR program for thermal cycling conditions for DNA amplification

Step	**Temperature** (°C)	**Time**	**Number of cycles**
Initial denaturation	95	2 min	1 cycle
Denaturation	95	0.5-1 min	
Annealing	42-65	0.5-1 min	25-35 cycles
Extension	72	1 min/kb	
Final extension	72	5 min	1 cycle
Soak	4	Infinite	1 cycle

Table 7. List of primers for mouse and human genes

Gene name	**Forward Primer from 5´ to 3´**	**Reverse Primer from 5´ to 3´**	**Annealing Temperature (°C)**
Mouse			
Plod1	CAGGAGGTGTTCATGTTCCT	CTCATGATAGTGTGTGAGCC	63
Plod2	AGTCGAGCAGCCTTGTCCAG	TCCTTCGTGCAAATGTGTGA	63
Plod3	GAGAACAGTACATTCACGAG	GACACCATGATGTATCGAGT	63
Tgm1	TCTACATGAAGTATGACACA	CACCTCGATATGCCATAGGT	57
Tgm2	GAGCGAGATGATCTGGAACT	ACTTCAGCTTGTCACACTGG	60
Hspa8	TTACCCGTCCCCGATTTGAAGAAC	TGTGTCTGCTTGGTAGGAATGG	58
Human			
PLOD1	ACATCCACCAGAACTACACC	GGATCGACGAAGGAGACTGC	60
PLOD2	CTGATGGATACTATGCACGA	AAGACATCTGGACAGGGCTG	60
PLOD3	GTGTTCTCGGGCAGTGACAC	GATCACACAGTCGTAGCGCA	60
TGM1	TGGTCTACATGAAGTACGAC	GAGATGCCATAGGGATGGTC	63
TGM2*(1)	GCAGCAGCCCCGTCTACGTG	GCTCTCGAAGTTCACCACCA	63
(2)		CAAGATCCCATTGTAGCTGA	63
HSPA8	TTACCCGTCCCCGATTTGAAGAAC	TGTGTCTGCTTGGTAGGAATGG	58

* Two different reverse primers for the TGM2 gene have been described in human cells. Both were used in the present study.

The semiquantitative PCR was carried out using either mouse primers for whole lung tissue and mouse fibroblasts or human primers for human paSMC or human keratinocytes. All primers used are listed in Table 7.

After the final extension, the sample was chilled down to 4 °C. Thereupon, the samples underwent analysis by gel electrophoresis or were stored at -20 °C.

3.2.8 Gel electrophoresis

Gel electrophoresis is used to separate nucleic acids or proteins, for example by size, physical structure or electric charge.

3.2.8.1 DNA gel electrophoresis

For DNA gel electrophoresis a 1% agarose gel was employed. The agarose powder was dissolved in 200 ml 1× Tris-acetate-EDTA (TAE) buffer (40 mM Tris-acetate, pH 8.0, 1 mM EDTA, pH 8.0). To melt the agarose, the mixture was heated in the microwave. To later visualize the DNA in the gel, 0.5 µg/ml ethidium bromide was added to the liquid gel. Ethidium bromide intercalates between DNA bases and fluoresces under UV light, whereby it can be seen and documented. The signal intensity correlates with the amount of DNA in the gel and, hence, is interpreted as a function of amplicon abundance. After 10 min cooling at room temperature, the gel solution was poured into a casting frame. While the gel was still in liquid form, the teeth of a plastic comb were inserted to form the wells. After at least 30 min at room temperature, the gel set and the comb could be carefully removed. The gel was transferred to another tray with a positive and a negative electric pole. The tray was filled with 1× TAE buffer and the samples along with the loading dye (containing 0.01% bromphenol blue, 40% glycerol in 1× TAE buffer) were loaded into the wells. The electrophoresis was performed by applying 100-120 V to the gel slab for 40-60 min. Thereafter the gel was examined under an UV light (λ=257 nm) transluminator and the signal was documented with a *Kodak 1D 3.5* camera for several different exposure times.

3.2.8.2 Protein gel electrophoresis

In order to separate out proteins in complex mixtures, a *sodium dodecyl sulfate (SDS) poly acrylamide gel electrophoresis (PAGE)* was performed. First, the

resolving (separating) gels had to be produced. The gel ingredients are listed in Table 8. The mixture was poured between two glass plates with spacers in between them. Isopropanol was layered on top of the gel solution to flatten the gel surface. Another gel, the *stacking gel,* the ingredients of which are listed in Table 9, was also poured between the glass plates on top of the *resolving gel,* in exchange for the isopropanol. A comb was placed into the *stacking gel,* while it was still in liquid form, to form the wells. Thereafter, the proteins extracted from mouse lung tissue were mixed with 2× loading dye buffer [100 mM Tris-Cl, pH 6.8, 200 mM DTT, 4% (vol/vol) SDS, 0.2% (vol/vol) bromphenol blue, 20% (vol/vol) glycerol, 9% β-mercaptoethanol] and denatured by heating to 95 °C for 10 min. The samples were loaded into the wells in the *stacking gel,* after having carefully removed the comb. The gel electrophoresis was run in 1× SDS-running buffer (25 mM Tris, 50 mM glycine, 0.1 % (vol/vol) SDS) for 1 h at 120 V.

Table 8. Resolving gel ingredients, and the corresponding amounts needed for 40 ml (4 gels).

Component	Volume
dH_2O	15.9 ml
30% Acrylamide	13.3 ml
1.5 M Tris-HCl, pH 8.8	10.0 ml
10% SDS	400 µl
10% APS	400 µl
TEMED	16 µl

APS = Ammonium persulfate
SDS = Sodium dodecyl sulfate poly acrylamide
TEMED = *N, N, N',N'* tetramethyl-ethane-1,2-diamine

Table 9. Stacking gel ingredients, and the corresponding amounts needed for 20 ml (4 gels).

Component	Volume
dH_2O	13.6 ml
30% Acrylamide	3.32 ml
1.5 M Tris-HCl, pH 6.8	2.52 ml
10% SDS	200 µl
10% APS	200 µl
TEMED	20 µl

APS = Ammonium persulfate
SDS = Sodium dodecyl sulfate poly acrylamide
TEMED = *N, N, N',N'* tetramethyl-ethane-1,2-diamine

3.2.9 Western blot analysis

The western blot or immunoblot is a technique used to detect, visualize and quantify proteins on a membrane by identifying these proteins with specific antibodies.

Following SDS-PAGE, the proteins that were separated in the gel were transferred on to a 0.25 µm nitrocellulose membrane: the membrane was placed on top of the gel, and filter paper placed on both sides to form a “sandwich” or stack. The entire stack was placed into a Bio-Rad chamber that contained blotting (transfer) buffer (25 mM Tris base, 192 mM glycine, 20% methanol). An electric potential of 110 V was applied to the chamber for 1 h. The electric current that was generated transferred the proteins from the gel to the nitrocellulose membrane.

After blotting, the membranes were placed in blocking solution (5% non-fat dry milk powder in PBS, 0.1% (vol/vol) Tween-20) for 1 h at room temperature. The blocking buffer was discarded and membranes were then incubated in blocking buffer containing the respective primary antibody against the target protein (primary and secondary antibodies and dilutions are listed in Table 10).

Table 10: Primary and secondary antibodies used in immunoblot-analysis.

Antibody	Host	Dilution	Company / Catalogue number
Primary antibodies			
LLH1 (Plod1)	Goat	1:200	Santa Cruz Biotech / sc-50062
LLH2 (Plod2)	Goat	1:200	Santa Cruz Biotech / sc-50067
Plod3	Rabbit	1:200	Protein Tech group / 11027-1-AP
TGase1 (Tgm1)	Goat	1:200	Santa Cruz Biotech / sc-18127
Anti-Transglutaminase Type II (Tgm2)	Goat	1:1000	Upstate / 06-471
α-tubulin	Rabbit	1:2500	Santa Cruz Biotech / sc-5286
Secondary antibodies			
Donkey anti-goat-HRP*-cong.		1:1000	Santa Cruz Biotech / sc-50062
Goat anti rabbit-HRP-cong.		1:3000	Pierce / 31460

* HRP = Horseradish peroxidase

This incubation was performed either at room temperature for 1 h or overnight at 4 °C. Antibodies and blocking solution were discarded and membranes were rinsed in washing buffer (1× PBS, 0.1% (vol/vol) Tween-20) 3×10 min, each time exchanging the buffer. This was followed by (depending on the host of the primary antibody) the application of goat or rabbit secondary horseradish peroxidase (HRP)-conjugated antibody (Table 10) in a dilution of 1:1000 or 1:3000 at room temperature for 1 h. Thereafter, membranes were again rinsed in washing buffer, this time 5×10 min each, using fresh washing buffer for every cycle. Membranes were then wetted with a mixture containing a 1:1 amount of peroxidase- and light sensitive enhancer-solution. The luminescence of the antibody-linked peroxidase reaction was documented on hyperfilm ECL (Kodak) in a darkroom.

The same membrane could be re-used for assessment of the expression of other proteins: For this purpose, the membrane was placed into washing buffer (1×5 min). Then the proteins were stripped off the membrane by placing the membrane in stripping buffer (100 mM β-mercaptoethanol, 62.5 mM Tris-Cl pH 6.8, 2% (mass/vol) SDS) at 50 °C for 30 min. Thereupon, the membrane was washed in washing buffer (2×5 min) and then blocked in blocking buffer for 1 h. The membrane could now be re-used for the detection of proteins.

3.2.10 Immunohistochemistry

Expression and location of Plod and Tgm protein and the γ-glutamyl-ε-lysine crosslink was assessed on 3-µm tissue sections, prepared as described above (*Processing of lung tissue*). Immunohistochemical analysis was performed using a Histostain-SP Kit. The whole-lung sections were deparaffinized by placing them in xylene 3×10 min. After that, sections were dehydrated in 100% ethanol 2×5 min, 95% ethanol 2×5 min, 70% ethanol 2×5 min, and 1×PBS 2×5 min. After antigen retrieval, performed by incubating the slides for 20 min at 100 °C in a pressure cooker in 6.5 mM sodium citrate, pH 6.0, the endogenous peroxidase activity was quenched with 3% (vol/vol) H_2O_2 for 10 min. The sections were blocked for 10 min at room temperature using a blocking solution provided in the kit. After that, the primary antibodies (Table 11) were applied to the sections and incubated overnight at 4 °C.

The primary antibody concentration varied depending on the type of antibody that was employed (Table 11). On the sections that served as negative control, no primary antibody was introduced, and sections were solely incubated with Tris buffer (“no primary” control), unless a competing peptide or protein was available, which was the case for Plod1, Plod3, and Tgm1 (Table 11). The next day, before applying the secondary antibodies (Table 11) to the sections, the slides were washed in 1× PBS 2×5 min. The sections were then incubated with a biotinylated secondary antibody for 10 min. The secondary antibody-solution was then removed and the slides were washed in 1× PBS 2×5 min. Streptavidin-conjugated HRP was applied to the sections for 10 min followed by chromogenic substrate for 1-10 min. After that, slides were rinsed again in 1× PBS for 2 min followed by counterstaining with Mayer’s hematoxylin. Staining of the sections was examined and photographed under an Olympus BX51 microscope.

Table 11: Primary and secondary antibodies used in immunohistochemistry.

Antibody	**Host**	**Dilution**	**Company/ Catalogue number**
Primary antibodies			
LLH1 (Plod1)	Goat	1:10	Santa Cruz Biotech/ sc-50062
LLH2 (Plod2)	Goat	1:25	Santa Cruz Biotech/ sc-50067
Antibody to PLOD3	Rabbit	1:25	Proteintech Group, Inc/ 11027-1-AP
TGase1 (Tgm1)	Goat	1:15	Santa Cruz Biotech/ sc-18127
Anti-Transglutaminase Type II (Tgm2)	Goat	1:50	Upstate/ 06-471
N-ε-γ-glutamyl Lysine	Mouse	1:100	Abcam/ Ab424
Secondary antibodies			
Biotinylated antibody to mouse		Ready-To-Use	Invitrogen/ 95-6543B
Biotinylated antibody to rabbit		Ready-To-Use	Invitrogen/ 95-6143B
Biotin-XX rabbit anti-goat-IgG		1:1000	Invitrogen/ A10518
Competing peptides/proteins			
Plod1 peptide			Santa Cruz Biotech/ SC-50062P
Plod3 GST-fusion			Proteintech Group, Inc/ Ag1480
Tgm1 peptide			Santa Cruz Biotech/ SC-18127P

Chapter 4

Results

4.1 Expression of lysyl hydroxylases and transglutaminases is dysregulated by hyperoxia *in vivo*

Neonatal mice that breathed 85% oxygen demonstrated an up-regulation of ECM cross-linking enzyme mRNA levels (Fig. 6) in lung tissues. Gene (mRNA) expression levels were assessed by semi-quantitative PCR and exhibited elevated levels for Plod1 (Fig. 6A) starting after 7 to 14 days of postnatal hyperoxia exposure. Similarly, Plod2 mRNA levels (Fig. 6A) were up-regulated from P14, while Plod3 mRNA levels (Fig. 6A) were evenly expressed throughout the observed time-period with a slight signal enhancement after 28 days of exposure to hyperoxia. Transglutaminase 1 (Fig. 6B) demonstrated a clear increase in gene-expression from P14 onward. As expected, since Tgm2 is a marker for lung maturation, mRNA levels of Tgm2 (Fig. 6B) increased with postnatal age. However, except for a subtle signal enhancement at P7, effects of hyperoxia on Tgm2 gene expression were not evident.

Protein-expression in mouse lung tissue was assessed by western blot (Fig. 7). Assessment of Plod1 protein expression (Fig. 7A), confirmed the pattern seen in mRNA expression and, exhibited increased signals at P21 and P28 in tissues from hyperoxia-exposed pups compared to tissues from control pups maintained for the same period of time under normoxic conditions. Plod2 exhibited increased protein abundance throughout the first 28 days of life under hyperoxia (Fig. 7A). The Plod3 protein abundance (Fig. 7A) was slightly elevated over the first two weeks under hyperoxic conditions, but at P28 was a down-regulated compared to the room-air control pups. A similar tendency could be seen in the protein expression levels of Tgm1 (Fig. 7B): up-regulation in the early stages (P7-P14) and slight down-regulation towards adulthood (P28). These trends are not consistent with the gene expression findings. It is noteworthy that the so-called *keratinocyte transglutaminase* (Tgm1) is expressed in the lung. Transglutaminase 2 (Fig. 7B) protein was expressed from two alternatively-spliced mRNA species. Although no effect of hyperoxia on mRNA levels

was observed, the Tgm2 protein was more abundant in hyperoxia-exposed lungs. While the reason for this is not immediately apparent, it may well be that hyperoxia can stabilise Tgm2 protein, resulting in an increased abundance.

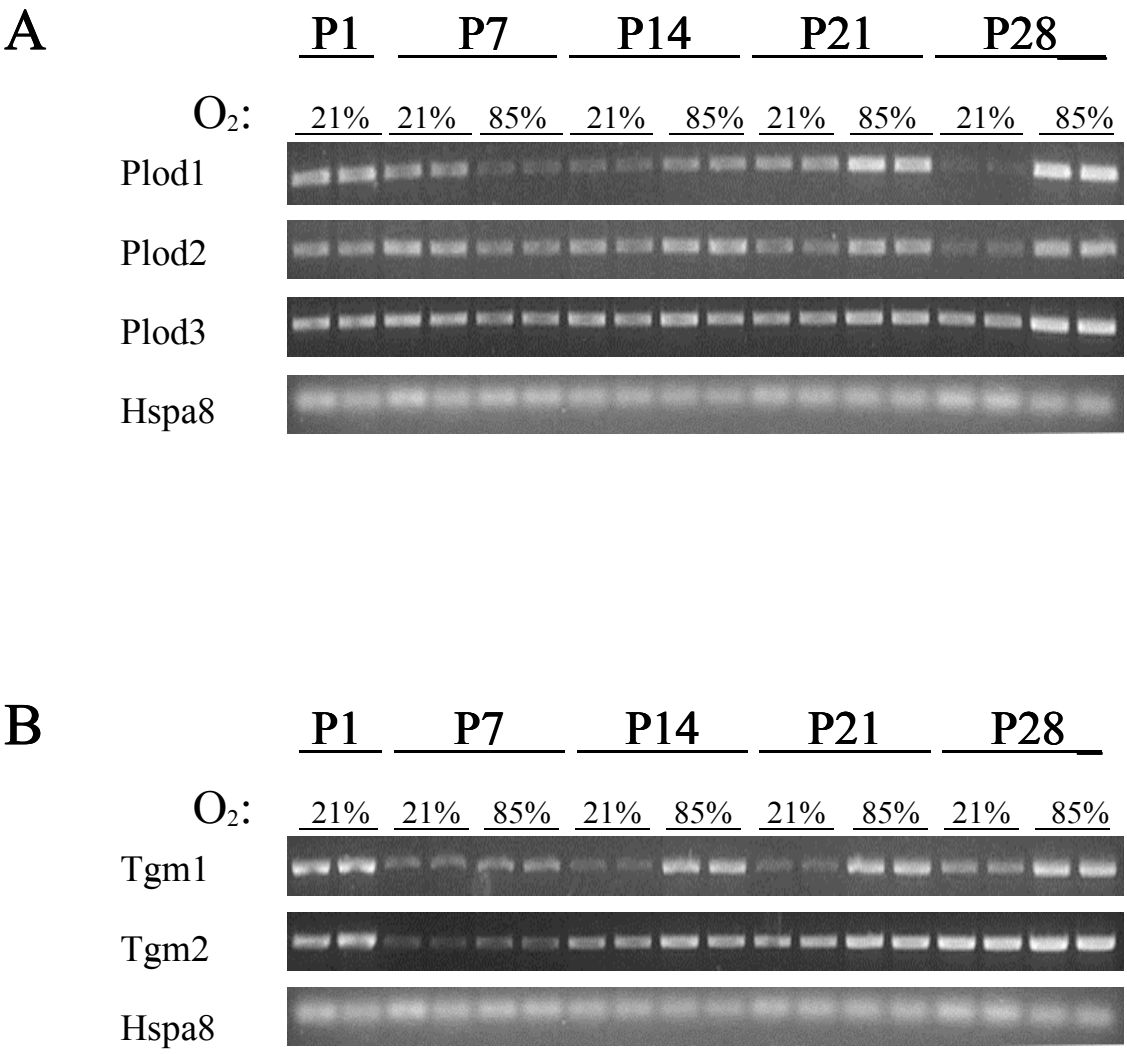

Figure 6. Gene expression profiles for (A) lysyl hydroxylases (Plod1, Plod2, Plod3) and (B) transglutaminases (Tgm1, Tgm2). The mRNA from the lungs of mouse pups exposed to 21% O_2 or 85% O_2 was monitored by semi-quantitative reverse transcriptase-polymerase chain reaction over the first month of postnatal life. The constitutively-expressed Hspa8 gene served as a control for loading equivalence.

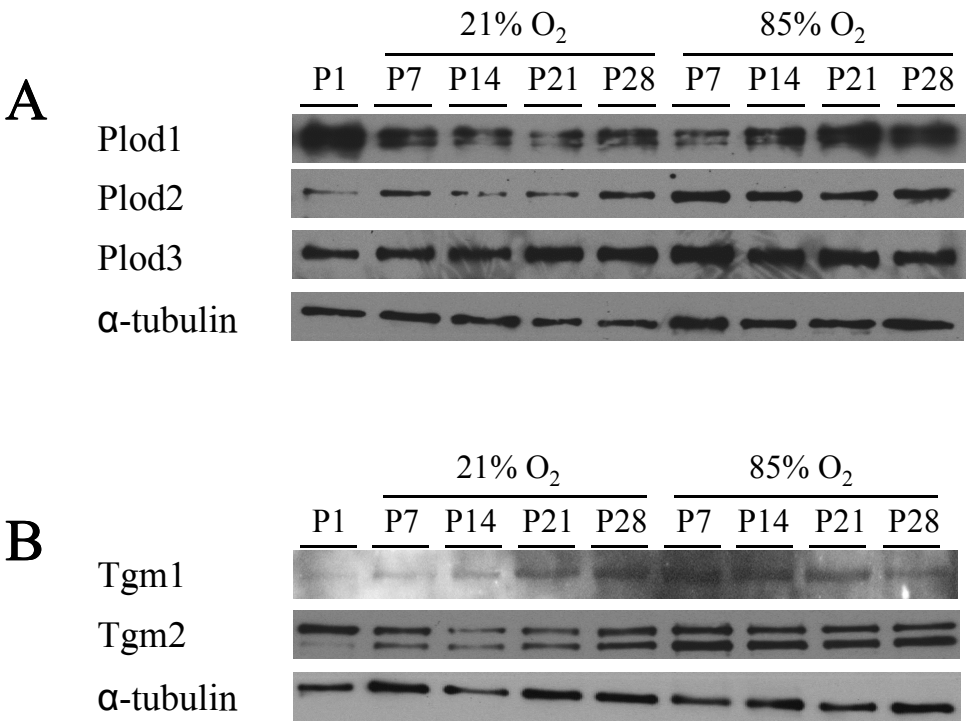

Figure 7. Protein expression of (A) lysyl hydroxylases (Plod1, Plod2, Plod3) and (B) transglutaminases (Tgm1, Tgm2) in mouse lung tissue was monitored by immunoblot analysis between postnatal day 1 and 28 (P1, P7, P14, P21, P28). Lungs were harvested from mice breathing 21% or 85% O_2. The constitutively-expressed α-tubulin was used as a loading control.

4.2 Inducibility of Plod- and Tgm-expression by hyperoxia and/or TGF-β-stimulation in different cell types

In order to locate where exactly in the lung the dysregulation of Plod and Tgm expression took place, it was necessary to examine specific cell lines. Moreover, the response of the cell lines to hyperoxia and TGF-β was assessed. Mouse lung fibroblasts (NIH/3T3), human keratinocytes (HaCaT) and human paSMC mRNA were monitored by semiquantitative PCR for changes in Plod and Tgm gene expression after having stimulated the cells with either 85% O_2 and TGF-β, separated or together for 24 h (Fig. 8). The Plod gene expression (Fig. 8A) was evident in all three cell lines, but was not altered by TGF-β and/or hyperoxia exposure except for Plod2 mRNA levels, which were slightly elevated in keratinocytes after TGF-β stimulation. However, no differences were evident when cells were treated with TGF-β and

85% O_2 or with TGF-β alone. As expected, Plod2 presented as two alternatively-spliced isoforms after transcription, evident as a double-band by semi-quantitative RT-PCR. However, this only occurred in human keratinocytes and has not been described before. Up to now, the appearance of both splice-isoforms has only been described in human kidney, spleen, liver and placenta.

Transglutaminase 2 mRNA expression (Fig. 8B) was also, but more markedly, up-regulated after one day of TGF-β treatment in keratinocytes and, again, exhibited no dysregulation caused by hyperoxic conditions. No changes could be seen in Tgm1 gene-expression, which was only present in keratinocytes. Transglutaminase 1, also known as the keratinocyte transglutaminase, is a cell-specific enzyme. In order to study the effects on a cell-line that definitely contains Tgm1, keratinocytes, although not typically lung cells, were also investigated. The analysis of the mouse whole-lung tissue demonstrated that Tgm1 is present in the lung. The analysis of the cell-lines demonstrated that Tgm1 is neither present in mouse fibroblasts nor paSMC. This raises the question whether keratinocytes are actually present in the lung or whether there is a different cell type, which was not investigated here, that expresses Tgm1. As mentioned already in the *Introduction,* Tgm1 has been described in normal bronchial epithelium. These cells should be investigated concerning Tgm1 expression under hyperoxia and TGF-β influence. As described in *Materials and Methods* TGM2 has two different reverse primers in human cells, hence, there is TGM2a and TGM2b. Interestingly, no TGM2b expression is found in human paSMC.

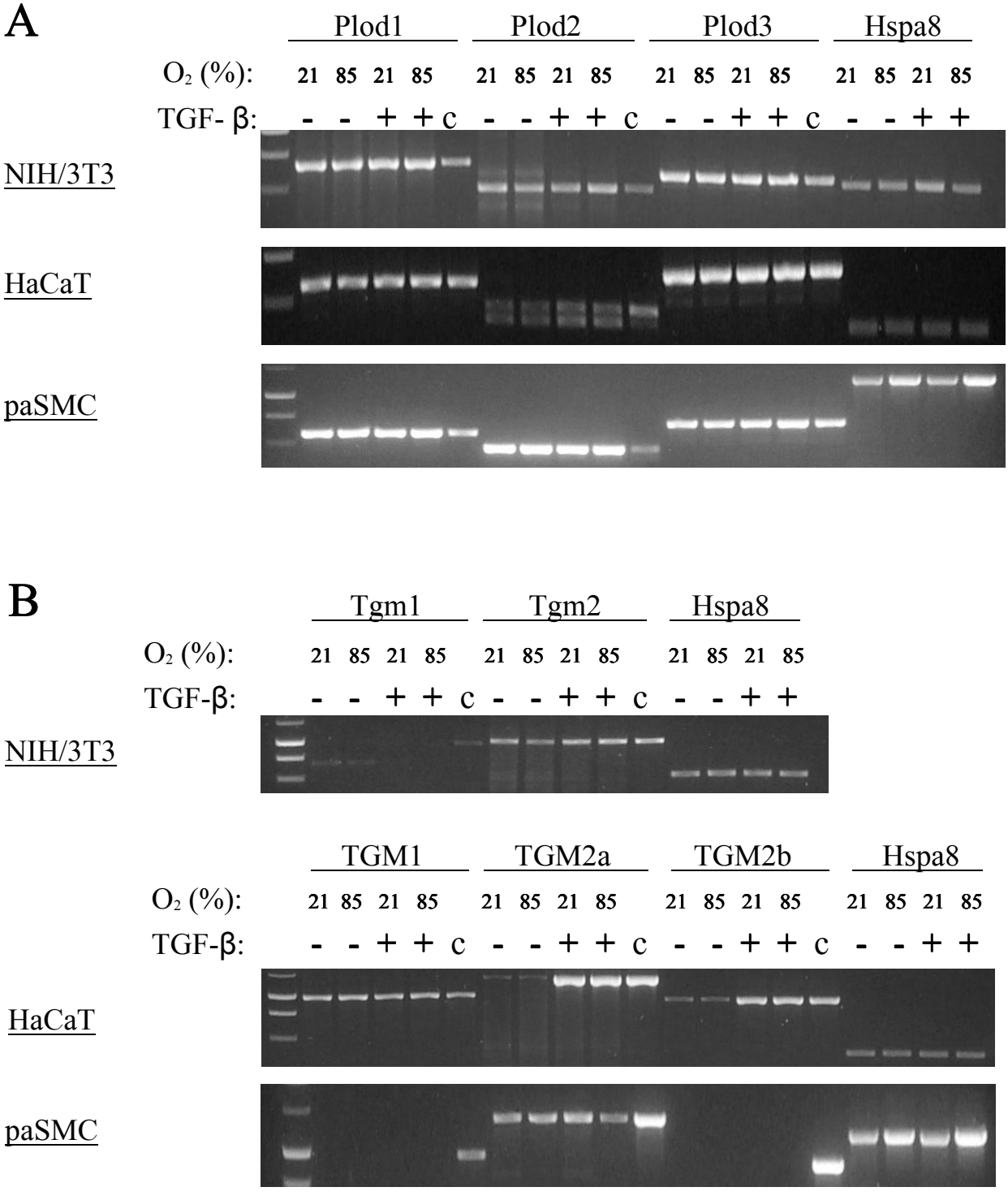

Figure 8. Different cell types were treated with either TGF-β1, hyperoxia or both for 24 h. Expression of (A) lysyl hydroxylases (Plod1, Plod2, Plod3) and (B) transglutaminases (Tgm1 and Tgm2) mRNA was then monitored by semiquantitative reverse transcriptase-polymerase chain reaction. The lane on the right of each gene was filled with cDNA from whole lung tissue and was used as an expression control (c). The Hspa8 gene served as loading control.

4.3 Localization of lysyl hydroxylases and transglutaminases in lung tissue of newborn mice

Localization of lysyl hydroxylases, transglutaminases and the γ-glutamyl-ε-lysine cross-link in the lungs of mouse pups was assessed by immunohistochemistry (IHC). Lung tissue was harvested from newborn mice at different postnatal days. Lysyl hydroxylase was detected in mouse lung tissue at P28 (Plod1) and P7 (Plod2 and Plod3) (Fig. 1). Transglutaminases were assessed in mouse lung tissue at P7 (Tgm1) and P14 (Tgm2) (Fig. 2). The enzymes were assessed in tissue at a postnatal age that was most appropriate (based on immunoblot analyses) to demonstrate differences in the intensity of staining between hyperoxia- *versus* normoxia-exposed lungs. However, here, IHC was primarily done to determine the exact location of Plods and Tgms in lung tissue, as this technique is generally not suitable to quantify protein expression.

Plod1 demonstrated a cell-specific expression pattern in the lung tissue of newborn mice: At P28 Plod1 was mainly localized in the walls of the pulmonary vessels. With regard to the results of the mRNA expression analysis in the cell lines, one would expect a more broad localization. This may be explained by the timepoint of assessment, as towards adulthood the distribution profiles of Plods become more specialized. Earlier in development, at P7 (data not shown), staining was also evident in the septa. Moreover, staining at P7 was more pronounced under normoxia than under hyperoxia, as indicated by gel PCR and western blot. However, it must be kept in mind that IHC is not a quantitative technique. The staining at P28, in contrast, was accentuated in the tissue that was exposed to chronic hyperoxia which, again, is consistent with the findings from the semiquantitative PCR and the western blots.

Plod2, protein expression of which was demonstrated to be up-regulated by hyperoxia throughout the first postnatal month, was examined for tissue localization at P7. Localization was mainly limited to the septa. Moreover, very little staining could be observed in paSMC and airway muscle (not shown). Again staining was more pronounced in tissue under chronic hyperoxia.

Plod3 was studied in tissues at P7 and was located very specifically at the septal junctions. This confirms earlier findings, that described pulmonary Plod3 as being cell

specific for type II pneumocytes. As expected, elevated O_2 levels did not obviously influence Plod3 expression.

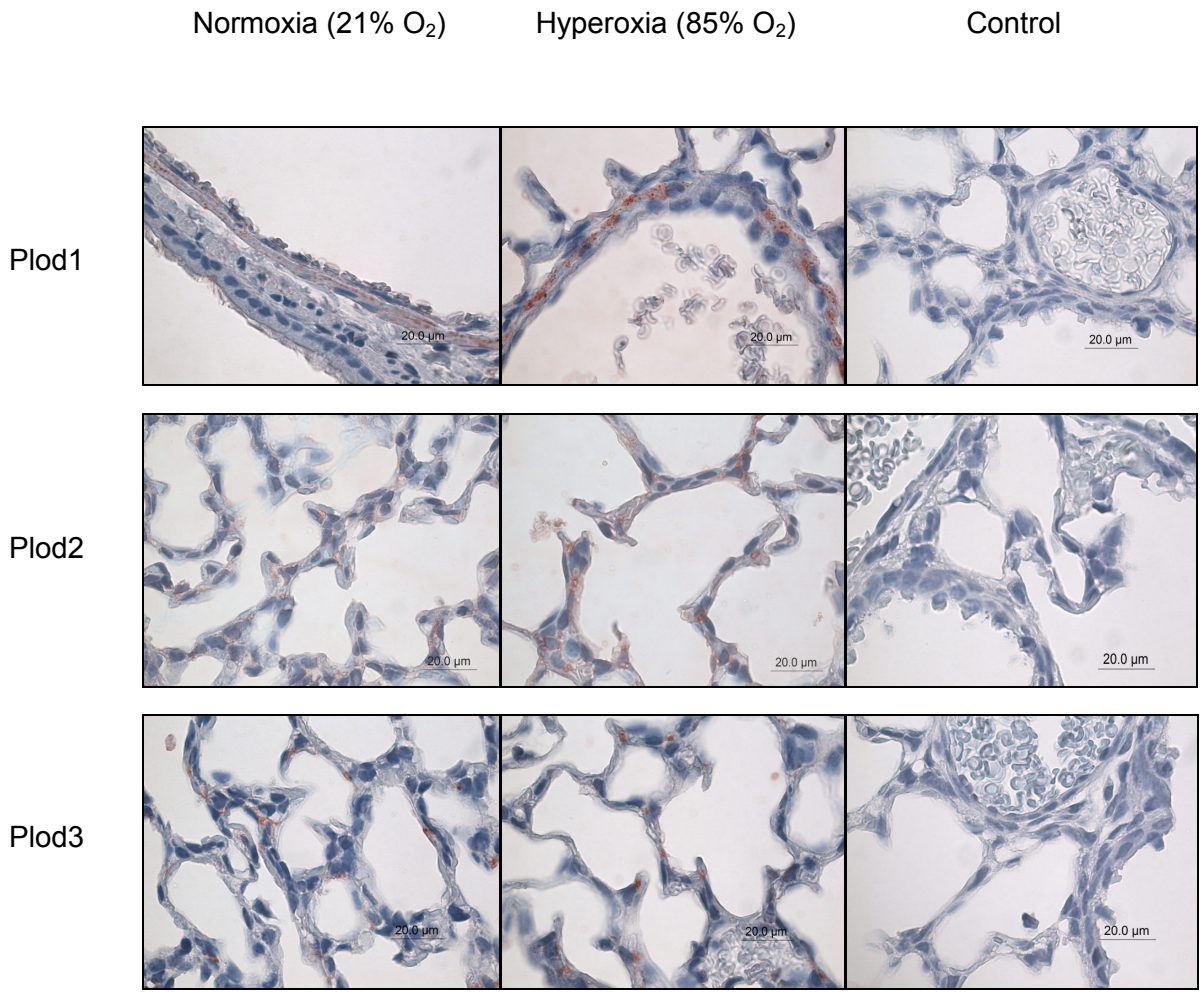

Figure 9. Localization of lysyl hydroxylases in lung tissue of newborn mice exposed to either hyperoxia (85% O_2) or normoxia (21% O_2). Sections were prepared from mouse lungs at P28 (Plod1) and P7 (Plod2 and Plod3) and assessed for localization of the respective enzyme. Control sections were solely incubated with Tris buffer.

The staining of Tgm1 was of particular interest as the enzyme has been described in lung tissue previously and, in the present study, was detected in the whole lung tissue of mice by RT-PCR and western blot, but was found in neither mouse lung fibroblasts nor paSMC. Here, the IHC revealed strong staining only at the junctions of the alveolar septa near the type II pneumocytes. If at all, there was faint staining in

the bronchial epithelium. The sections were taken from mice at P7, as in the western blot analysis dysregulation by hyperoxia was most evident at that time-point. Again, this was reproducible by IHC, where the staining appeared more pronounced under hyperoxia.

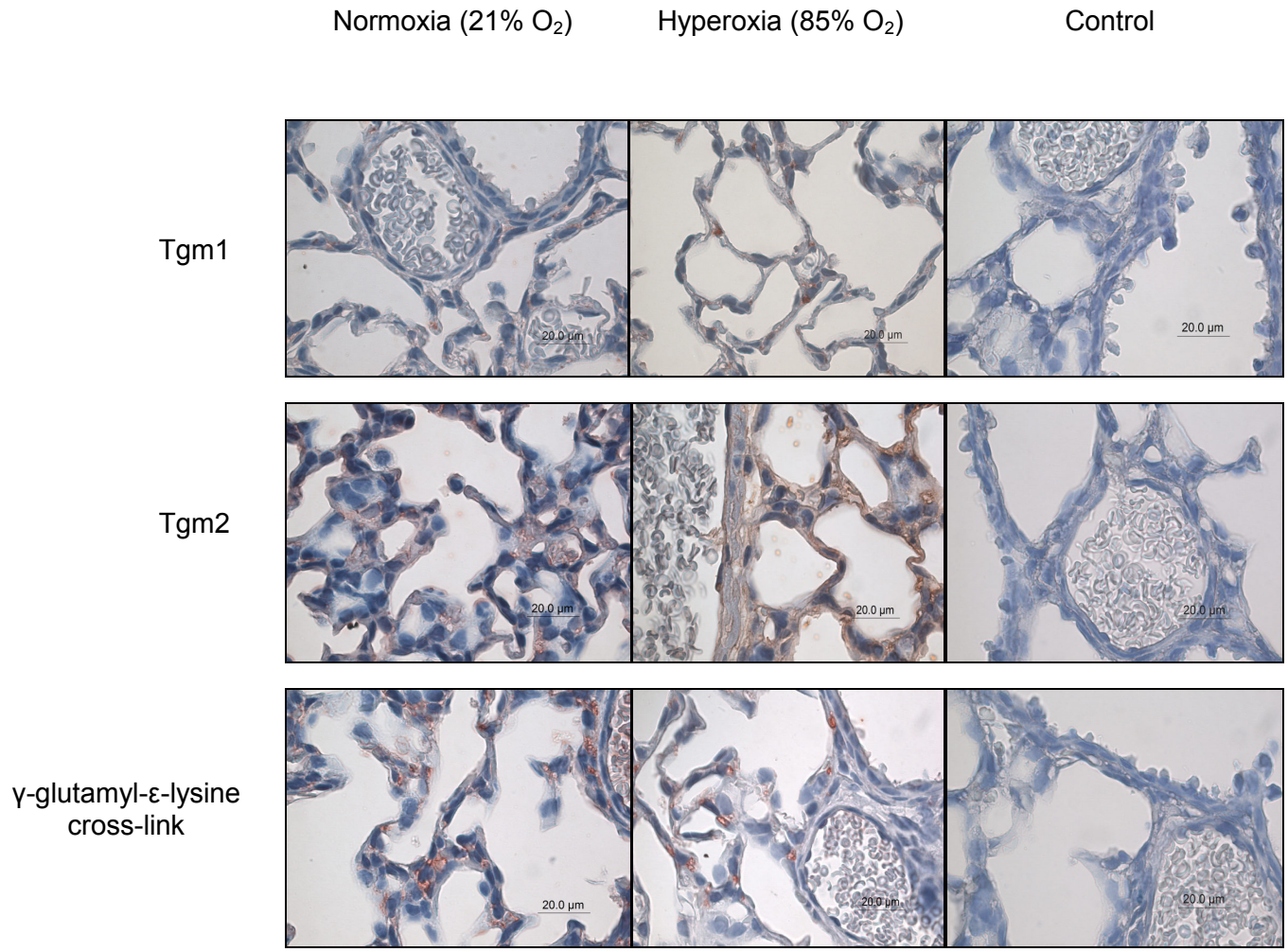

Figure 10. Localization of transglutaminases and the γ-glutamyl-ε-lysine cross-link in lung tissue of newborn mice exposed to either hyperoxia (85% O_2) or normoxia (21% O_2). Sections were prepared from mouse lungs at P7 (Tgm1), P14 (Tgm2) and P7 (cross-link) and assessed for localization of the respective enzyme. Control sections were solely incubated with Tris buffer.

Sections for Tgm2 staining were obtained from pups at P14 and demonstrated overall stronger staining in lung tissue that was exposed to hyperoxia. Transglutaminase 2 was mainly localized in alveolar septa and vascular endothelial

cells. There was also faint staining noted in the bronchial epithelium. In contrast to the paSMC *in vitro* data, paSMC were, if at all, very weakly stained.

Staining for the γ-glutamyl-ε-lysine cross-link was assessed at P7. The localization of this product of the Tgm-catalyzed reaction, which is highly resistant to proteolysis, may hint towards important conclusions about the pathomechanism of the disturbed septation in BPD. Consistent with the location of the Tgms, the cross-link was found in the junctions of the alveolar septa close to the type II pneumocytes. Increased cross-linking of the pulmonary type I and type III collagen at these locations, which are crucial for the development of the blood-air barrier, may lead to the characteristic disturbance of septation and lung function in BPD. However, a clear increase in staining intensity in lung tissue exposed to hyperoxia versus tissue exposed to normoxia could not be seen at P7. As IHC is not a quantitative technique, this should not be overinterpreted.

Chapter 5

Discussion

Proper branching of the airways and secondary septation are crucial for normal lung development, as these processes occur mainly during late lung development and are highly dependent on proper ECM production and remodeling[74]. In important developmental lung diseases such as BPD, ECM remodeling and deposition have been demonstrated to be disturbed. The exact pathogenic mechanisms, however, remain poorly understood. While several studies performed to date have focused on the production of ECM proteins in BPD, few have addressed the subsequent remodeling of these proteins. The dynamics of ECM remodeling is impacted by the establishment and breakdown of the intra- and inter-molecular cross-links of the ECM proteins. Enzymes that cross-link ECM proteins have been identified previously and the expression of these enzymes has been demonstrated to be dysregulated in animal models of BPD[75]. However, there have been inconsistent findings reported previously regarding the regulation of ECM cross-linking enzymes by hyperoxia: Lysyl oxidase eypression was down-regulated in a rat model of BPD[76], using 95% O_2 to create hyperoxic conditions, whereas lysyl oxidase expression was up-regulated in a mouse model of chronic exposure to hyperoxia of 85% O_2[38].This divergence may be explained by different oxygen-concentrations used in the two animal models, or by the differing response to high oxygen concentrations displayed by mammals, even between different mouse strains[77].

In this study, two families of enzymes that are known to be important for ECM stability were assessed with respect to responses to hyperoxia, using a mouse model of BPD: the lysyl hydroxylases (Plod1, Plod2, Plod3) and the transglutaminases (Tgm1, Tgm2). So far, Plods and Tgms have not been examined concerning their role in the pathogenesis of BPD. With reference to the trend-setting studies mentioned above that suggest dysregulation of ECM crosslinking enzymes, in this study it was hypothesized that Plod and Tgm expression is also dysregulated in BPD.

The data presented here demonstrate the up-regulation of expression of three collagen cross-linking enzymes (Plod1, Plod2, Tgm1) at the mRNA level and the up-regulation of expression of three enzymes (Plod1, Plod2, Tgm2) at the protein level in newborn animals with hyperoxic lung injury and perturbed ECM structure. Although the up-regulation at the gene and protein levels under hyperoxic conditions are not completely consistent with each other, the trend that can be seen supports the hypothesis of the "over-stabilized" ECM in BPD. The expression of the lysyl hydroxylases Plod1 and Plod2 are up-regulated consistently at the mRNA level as well as at the protein level by chronic hyperoxia. Transglutaminase 1 expression, however, was up-regulated by hyperoxia at the gene expression level, but not at the protein expression level, whereas Tgm2 expression was up-regulated at the protein-level by hyperoxia, but not at the gene-level. The reason for this divergence is not completely clear, but may be explained by additional control mechanisms before or after translation. With regard to the pathogenesis of BPD, the protein levels of the ECM cross-linking enzymes, as they reflect the regulation of the executive enzymes, have a higher importance than the gene expression levels.

The localization of the Plods, Tgms and the the γ-glutamyl-ε-lysine cross-link was assessed in lung tissue from newborn pups by IHC. This experiment was carried out to detect the location in the lung where the hypothesized pathological cross-linking occurs. Time points of assessment were chosen according to when the clearest changes of protein production were evident in the western blot analysis. Intensity of staining was, except for the cross-link and Plod3, always increased by hyperoxia. This is consistent with the results from the western blots. However, as IHC is not a quantitative technique and it should not be used as such. All proteins were localized in the septa, which supports the hypothetical role of these enzymes in the pathomechanism of disturbed septation in BPD.

Up-regulation of expression of enzymes of the Plod family, which are broadly and highly expressed during lung development, may lead to extensive consequences for ECM assembly of the immature lung. Increased Plod1 levels may lead to an increased hydroxylysine/lysine ratio in the helical collagen structure and may explain the "*tortuous*" appearance of the collagen fibers that was observed in infants with chronic lung disease[37]. The consequences of alterations to lysyl hydroxylase abundance can be well observed in Plod1-/- mice that demonstrate decreased

hydroxylysine content in all tissues, degenerated smooth muscle cells, and abnormal collagen morphology[78]. The main cause of death in these mice was aortic aneurysms due to gradual deterioration of the aortic wall, as observed by ultra-structural analysis. These data suggest a key role for this family of enzymes in the development of the ECM. However, an analysis of pulmonary ECM in these mice was not performed.

In 2003 a study from van der Slot *et al.* demonstrated that the collagen deposited in fibrotic tissue contained increased levels of Plod2 mRNA and of the pyridinoline cross-link, which derives from hydroxylated lysine residues. By analyzing the genetic defect of Bruck's syndrome, which is charcterized by pyridinoline deficiency, it could be concluded that the pyridinoline cross link is the result of Plod2 enzyme activity. Hence, it was postulated that elevated Plod2 levels are, at least in part, responsible for tissue fibrosis[79]. Additionally, two years later, a study demonstrated that the profibrotic Plod2b as well as the pyridinoline cross-link are induced by various cytokines including all three isoforms of TGF-β, IL-4, activin A, and tumor necrosis factor (TNF)-α in normal skin fibroblasts[56]. Given these results, pulmonary Plod2b upregulation, as seen in the present study, may lead to fibrotic changes in collagen deposition and remodeling in the lung as a result of increased TGF-β signaling under chronic hyperoxia. However, Plod2 mRNA expression was not enhanced in mouse lung fibroblasts and human paSMC after one day of TGF-β1 stimulation. This may be due to insufficient stimulation time, which was limited by the survival time of the cells. However, a slight upregulation of Plod2 mRNA levels could be seen in human keratinocytes. The assessment of keratinocytes was performed as a control and would only be of interest regarding BPD, if keratinocytes were present in the lung.

Transglutaminase1, although primarily known to be present in keratinocytes, has been described to be expressed in the bronchial epithelium[61]. The IHC in the present study, however, demonstrates a specific Tgm1 presence in the septal junctions around the type II pneumocytes and only weak staining in the bronchial epithelium. Presence of Tgm1 in pneumocytes has not been described before and should be examined more closely in pneumocyte cell lines. The crosslink built by Tgm1 activity is highly resistant to proteolysis and, if prematurely up-regulated in the lung within the first two postnatal weeks under chronic hyperoxia, as seen in the immunoblot analysis, may lead to irreversible damage to normal pulmonary development. This

mechanism, however, is highly speculative, as, to date, there is very little known about the role of pulmonary Tgm1.

Transglutaminase 2, in contrast, has been extensively examined in the lung and is known to have profibrotic activity in the lung. The latest publication on this topic demonstrated Tgm2 involvement in pulmonary fibrosis in a mouse model, the importance of Tgm2 for normal lung fibroblast function, and Tgm2 inducibilty by TGF-β[80]. The early and constant up-regulation of Tgm2 by chronic hyperoxia may, hence, lead to early, excessive scar tissue formation by irreversible ECM crosslinking. Taking into consideration that Tgm2 can be used as a marker for lung development[81], this may be interpreted as an early arrest of lung maturarion through oxygen-toxicity. Definite enhancement of Tgm2 mRNA expression can be seen after one day of TGF-β1 stimulation in human keratinocytes, but neither in human paSMC nor in mouse lung fibroblasts. This should be re-examined after longer exposure periods to TGF-β1 and in other pulmonary cell lines.

5.1 Conclusion

These data demonstrate two more families of dysregulated ECM crosslinking enzymes (in addition to lysyl oxidases) in a mouse model of BPD. The up-regulation of Plod and Tgm expression under chronic normobaric hyperoxia supports the hypothesis of a pathological “over-stabilization” of the ECM in BPD. However, more data need to be gathered regarding Plod and Tgm function in BPD.

Regarding the cytokine inducibility of Plods and Tgms, more experiments are needed in order to draw accurate conclusions: Apart from TGF-β1, more cytokines should be targeted, including for example IL-4, activin A, TNF-α and the other TGF-β subtypes. Other promising pulmonary cell lines could be examined regarding their cytokine inducibility, including bronchial epithelial cells, pneumocytes and vascular endothelial cells. Promoter-inducibility of the enzymes could be assessed by luciferase essay. In 2007, a study showed improved pulmonary alveologenesis and vasculogenesis in anti-TGF-β IgG1 antibody treated mice exposed to chronic hyperoxia[40]. Apart from being a possible treatment option in the future, these antibodies could be used to indirectly prove inducibility of Plods and Tgms: Antibody-treated mice should show decreased levels of Plod and Tgm expressions, if they are TGF-β inducible.

In summary, these two families of ECM enzymes that might play an important role in the pathogenesis of BPD provide more targets for further investigation and encourage looking for other dysregulated ECM cross linking families.

Chapter 6

Abstract

Bronchopulmonary dysplasia is a complication of premature birth characterized by impaired alveolar development. Remodeling of the ECM is a driving force for alveolarization and, if pertubated, may impair septation, suggesting dysregulation of ECM remodeling enzymes that drive collagen fiber formation and maturation: the procollagen-lysine, 2-oxoglutarate 5-dioxygenases (Plod) family, also known as lysyl hydroxylases (which catalyzes glycosylation and hydroxylation of collagen), and the transglutaminases Tgm1 and Tgm2, which cross-link ECM components.

Expressions of Plod1, Plod2, Plod3, Tgm1 and Tgm2 were determined using a popular mouse model of BPD, in which mouse pups are exposed to hyperoxia (85% O_2) or normoxia (21% O_2) for 28 days after birth. The lungs of these mice were harvested at various time-points and assessed for Plod and Tgm expression and localization by semi-quantitative RT-PCR, immunoblotting and immunohisto-chemistry. Increased expressions of Plods and Tgms could be observed at the gene and protein levels under hyperoxic conditions compared to normoxic conditions.

The data suggest that BPD is characterized by elevated levels of ECM-stabilizing molecules, which may make the ECM more resistant to remodeling. This over-stabilized state of the ECM may, at least in part, underlie the arrested septation observed both in the lungs of infants with BPD, and in animal models of BPD.

Chapter 7

Zusammenfassung

Bronchopulmonale Dysplasie ist eine Komplikation bei Frühgeborenen, welche durch eine fehlgesteuerte Entwicklung der Lungenalveolen charakterisiert ist. Der Umbau der ECM ist die treibende Kraft für die Bildung der Alveolen und kann, falls er behindert wird, zu einer Beeinträchtigung der alveolären Septierung führen. Dies lässt auf eine Fehlregulation der für den Umbau der ECM verantwortlichen Enzyme bei der Entstehung der BPD schließen: Die Prokollagen-Lysin, 2-Oxoglutarat 5-Dioxygenase (Plod) Familie, auch bekannt als Lysyl Hydroxylasen (welche die Glykosylierung und Hydroxylierung von Kollagenmolekülen katalysieren) und die Transglutaminasen Tgm1 und Tgm2, welche die ECM Komponenten quervernetzen.
Um die Expression von Plod1, Plod2, Plod3, Tgm1 und Tgm2 zu untersuchen, wurde ein gängiges Maus-Modell der BPD benutzt, bei dem neugeborene Mäuse in den ersten 28 postnatalen Tagen entweder hohen Sauerstoff-Konzentrationen (85% O_2) oder normalen Sauerstoff-Konzentrationen (21% O_2) ausgesetzt wurden. Die Lungen dieser Mäuse wurden zu verschiedenen Zeitpunkten entnommen und mittels semiquantitativer RT-PCR, Western-Blot und Immunhistochemie hinsichtlich der Plod- und Tgm-Expression und -Lokalisation untersucht.
Unter dem Einfluss von hohen Sauerstoffkonzentrationen konnte eine Steigerung der Plod- und Tgm-Expression sowohl auf Gen- als auch auf Proteinebene beobachtet werden, verglichen mit der Expression in der Kontrolle unter normalen Sauerstoffkonzentrationen.
Diese Daten deuten darauf hin, dass BPD durch eine gesteigerte Synthese von ECM-stabilisierenden Enzymen gekennzeichnet ist, was möglicherweise zu einer Behinderung des notwendigen Umbaus der ECM führt. Dieser „über-stabilisierte“ Zustand könnte, zumindest teilweise, der frühzeitigen Terminierung der alveolären Septierung zu Grunde liegen, welche sowohl in den Lungen der an BPD verstorbenen Kinder, als auch in BPD Tiermodellen beobachtet wurde.

Chapter 8

List of references

[1] Groothuis JR, Gutierrez KM, Lauer BA. Respiratory syncytial virus infection in children with bronchopulmonary dysplasia. Pediatrics 1988;82:199-203.

[2] Jobe AH, Bancalari E. Bronchopulmonary dysplasia. Am J Respir Crit Care Med 2001;163:1723-9.

[3] Giacoia GP, Venkataraman PS, West-Wilson KI, Faulkner MJ. Follow-up of school-age children with bronchopulmonary dysplasia. J Pediatr 1997;130:400-8.

[4] Schmidt B, Asztalos EV, Roberts RS, Robertson CM, Sauve RS, Whitfield MF; Trial of Indomethacin Prophylaxis in Preterms (TIPP) Investigators.. Impact of bronchopulmonary dysplasia, brain injury, and severe retinopathy on the outcome of extremely low-birth-weight infants at 18 months: results from the trial of indomethacin prophylaxis in preterms. JAMA 2003;289:1124-9.

[5] Jobe AH. The new bronchopulmonary dysplasia. Curr Opin Pediatr 2011;23(2):167-72.

[6] Northway WH Jr, Rosan RC, Porter DY. Pulmonary disease following respirator therapy of hyaline-membrane disease. Bronchopulmonary dysplasia. N Engl J Med 1967;276:357–368.

[7] Kramer BW, Lievense S, Been JV, Zimmermann LJ. [From classic to new bronchopulmonary dysplasia]. Ned Tijdschr Geneeskd 2010;154:A1024.

[8] Sankar MJ, Agarwal R, Deorari AK, Paul VK. Chronic lung disease in newborns. Indian J Pediatr 2008;75(4):369-76.

[9] Hislop AA, Wigglesworth JS, Desai R, Aber V. The effects of preterm delivery and mechanical ventilation on human lung growth. Early Hum Dev 1987;15(3):147-64.

[10] Hamrick SE, Hansmann G. Patent ductus arteriosus of the preterm infant. Pediatrics 2010;125(5):1020-30.

[11] Jobe AH, Ikegami M. Antenatal infection/inflammation and postnatal lung maturation and injury. Respir Res 2001;2(1):27-32.

[12] Hayes D Jr, Feola DJ, Murphy BS, Shook LA, Ballard HO. Pathogenesis of bronchopulmonary dysplasia. Respiration 2010;79(5):425-36.

[13] Wilson AC. What does imaging the chest tell us about bronchopulmonary dysplasia? Paediatr Respir Rev 2010;11(3):158-61.

[14] Walsh MC, Yao Q, Gettner P, Hale E, Collins M, Hensman A, Everette R, Peters N, Miller N, Muran G, Auten K, Newman N, Rowan G, Grisby C, Arnell K, Miller L, Ball B, McDavid G; National Institute of Child Health and Human Development Neonatal Research Network. Impact of a physiologic definition on bronchopulmonary dysplasia rates. Pediatrics 2004;114(5):1305-11.

[15] Christou H, Brodsky D. Lung injury and bronchopulmonary dysplasia in newborn infants. J Intensive Care Med 2005;20(2):76-87.

[16] Lemons JA, Bauer CR, Oh W, Korones SB, Papile LA, Stoll BJ, Verter J, Temprosa M, Wright LL, Ehrenkranz RA, Fanaroff AA, Stark A, Carlo W, Tyson JE, Donovan EF, Shankaran S, Stevenson DK.. Very low birth weight outcomes of the National Institute of Child Health and Human Development Neonatal Research Network, January 1995 through December 1996. Pediatrics 2001;107:e1-e8.

[17] Screiber MD, Gin-Mestan K, Marks JD, et al. Inhaled nitric oxide in premature infants with the respiratory distress syndrome. N Engl J Med 2003;349:2099-2107.

[18] Hislop AA. Airway and blood vessel interaction during lung development. J Anat 2002;201(4):325-34.

[19] Coalson JJ, Winter VT, Siler-Khodr T, Yoder BA. Neonatal chronic lung disease in extremely immature baboons. Am J Respir Crit Care Med 1999;160(4):1333-46.

[20] Bland RD. Neonatal chronic lung disease in the post-surfactant era. Biol Neonate 2005;88:181-191.

[21] Stenmark KR, Abman SH. Lung vascular development: implications for the pathogenesis of bronchopulmonary dysplasia. Annu Rev Physiol 2005;67:623-661.

[22] Thébaud B, Abman SH. Bronchopulmonary dysplasia: where have all the vessels gone? Roles of angiogenic growth factors in chronic lung disease. Am J Respir Crit Care Med 2007;175:978-985.

[23] De Paepe ME, Mao Q, Powell J, Rubin SE, DeKoninck P, Appel N, Dixon M, Gundogan F. Growth of pulmonary microvasculature in ventilated preterm infants. Am J Respir Crit Care Med 2006;173:204-211.

[24] Warner BB, Stuart LA, Papes RA, Wispe JR. Functional and pathological effects of prolonged hyperoxia in neonatal mice. Am J Physiol 1998;275(1 Pt 1):L110-7.

[25] Thibeault DW, Mabry SM, Ekekezie II, Zhang X, Truog WE. Collagen scaffolding during development and its deformation with chronic lung disease. Pediatrics 2003 Apr;111(4 Pt 1):766-76.

[26] Pierce RA, Albertine KH, Starcher BC, Bohnsack JF, Carlton DP, Bland RD. Chronic lung injury in preterm lambs: disordered pulmonary elastin deposition. Am J Physiol 1997;272(3 Pt 1):L452-60.

[27] Bland RD, Ertsey R, Mokres LM, Xu L, Jacobson BE, Jiang S, Alvira CM Rabinovitch M, Shinwell S, Dixit A. Mechanical ventilation uncouples synthesis and assembly of elastin and increases apoptosis in lungs of newborn mice. Prelude to defective alveolar septation during lung development? Am J Physiol Lung Cell Mol Physiol 2008;294(1):L3-14.

[28] Stephen E McGowan. Extracellular matrix and the regulation of lung development and repair. FASEB J 1992;6(11):2895-904.

[29] Bourbon J, Boucherat O, Chailley-Heu B, Delacourt C. Control mechanisms of lung alveolar development and their disorders in bronchopulmonary dysplasia. Pediatr Res 2005;57(5 Pt 2):38R-46R.

[30] Chetty A, Cao GJ, Severgnini M, Simon A, Warburton R, Nielsen HC. Role of matrix metalloprotease-9 in hyperoxic injury in developing lung. Am J Physiol Lung Cell Mol Physiol 2008;295(4):L584-92.

[31] Srisuma S, Bhattacharya S, Andalcio T, Simon DM, Arikan MC, Starcher B, Marian TJ. Fibroblast growth factor receptor signaling regulates extracellular matrix gene expression during alveogenesis. Proc Am Thorac Soc 2006;3:549-550.

[32] Verrechia F, Mauviel A. Transforming growth factor-beta signaling through the smad pathway: role in extracellular matrix gene expression and regulation. J Invest Dermatol 2002;118(2):211-5.

[33] Alejandre-Alcázar MA, Shalamanov PD, Amarie OV, Sevilla-Pérez J, Seeger W, Eickelberg O, Morty RE. Temporal and spatial regulation of bone morphogenetic protein signaling in late lung development. Dev Dyn 2007;236(10):2825-35.

[34] Kivirikko KI, Pihlajaniemi T. Collagen hydroxylases and the protein disulfide isomerase subunit of prolyl 4-hydroxylases. Adv Enzymol Relat Areas Mol Biol 1998;72:325-98.

[35] Wiestner M, Krieg T, Horlein D, Glanville RW, Fietzek P, Muller PK. Inhibiting effect of procollagen peptides on collagen biosynthesis in fibroblast cultures. J Biol Chem 1979;254:7016-23.

[36] Bailey AJ, Robins SP, Balian G. Biological significance of the intermolecular crosslinks of collagen. Nature 1974;251:105-9.

[37] Thibeault DW, Mabry SM, Ekekezie II, Zhang X, Truog WE. Collagen scaffolding during development and its deformation with chronic lung disease. Pediatrics 2003;111(4 Pt 1):766-76.

[38] Kumarasamy A, Schmitt I, Nave AH, Reiss I, van der Horst I, Dony E, Roberts JD Jr, de Krijger RR, Tibboel D, Seeger W, Schermuly RT, Eickelberg O, Morty RE. Lysyl Oxidase Activity Is Dysregulated during Impaired Alveolarization of Mouse and Human Lungs. Am J Respir Crit Care Med 2009;15;180(12):1239-52.

[39] Jankov RP, Keith Tanswell A. Growth factors, postnatal lung growth and bronchopulmonary dysplasia. Pediatr Respir Rev 2004;5Suppl A:S265-75.

[40] Nakanishi H, Sugiura T, Streisand JB, Lonning SM, Roberts JD, Jr. TGF-β-neutralizing antibodies improve pulmonary alveologenesis and vasculogenesis in the injured newborn lung. Am J Physiol Lung Cell Mol Physiol 2007;293:L151-161.

[41] Groenman F, Unger S, Post M. The molecular basis for abnormal human lung development. Biol Neonate 2005;87:164-177.

[42] Alejandre-Alcázar MA, Kwapiszewska G, Reiss I, Amarie OV, Marsh LM, Sevilla-Pérez J, Wygrecka M, Eul B, Köbrich S, Hesse M, Schermuly RT, Seeger W, Eickelberg O, Morty RE. Hyperoxia modulates TGF-β/BMP signaling in a mouse model of bronchopulmonary dysplasia. Am J Physiol Lung Cell Mol Physiol 2007;292:L537-L549.

[43] Puistola U, Turpeenniemi-Hujanen TM, Myllylä R, Kivirikko KI. Studies on the lysyl hydroxylase reaction. I. Initial velocity kinetics and related aspects. Biochim Biophys Acta 1980 11;611(1):40-50.

[44] Eyre D, Shao P, Weis MA, Steinmann B. The kyphoscoliotic type of Ehlers-Danlos syndrome (type VI): differential effects on the hydroxylation of lysine in collagens I and II revealed by analysis of cross-linked telopeptides from urine. Mol Genet Metab 2002;76(3):211-6.

[45] van der Slot AJ, Zuurmond AM, van den Bogaerdt AJ, Ulrich MM, Middelkoop E, Boers W, Karel Ronday H, DeGroot J, Huizinga TW, Bank RA. Increased formation of pyridinoline cross-links due to higher telopeptide lysyl hydroxylase levels is a general fibrotic phenomenon. Matrix Biol 2004;23(4):251-7.

[46] Brinckmann J, Kim S, Wu J, Reinhardt DP, Batmunkh C, Metzen E, Notbohm H, Bank RA, Krieg T, Hunzelmann N. Interleukin 4 and prolonged hypoxia induce a higher gene expression of lysyl hydroxylase 2 and an altered cross-link pattern: important pathogenetic steps in early and late stage of systemic scleroderma? Matrix Biol 2005;24(7):459-68.

[47] Ha-Vinh, R., Alanay, Y., Bank, R.A., Campos-Xavier, A.B., Zankl, A., Superti-Furga, A., Bonafé, L. Phenotypic and molecular characterization of Bruck syndrome (osteogenesis imperfecta with contractures of the large joints) caused by a recessive mutation in PLOD2. Ha-Vinh, R., Alanay, Y., Bank, R.A., Campos-Xavier, A.B., Zankl, A., Superti-Furga, A., Bonafé, L. Am J Med Genet A 2004;131(2):115-20.

[48] Wang C, Luosujärvi H, Heikkinen J, Risteli M, Uitto L, Myllylä R. The third activity for lysyl hydroxylase 3: galactosylation of hydroxylysyl residues in collagens *in vitro*. Matrix Biol 2002;21(7):559-66.

[49] Salo AM, Wang C, Sipilä L, Sormunen R, Vapola M, Kervinen P, Ruotsalainen H, Heikkinen J, Myllylä R. Lysyl hydroxylase 3 (LH3) modifies proteins in the extracellular space, a novel mechanism for matrix remodeling. J Cell Physiol 2006;207(3):644-53.

[50] Myllylä R, Wang C, Heikkinen J, Juffer A, Lampela O, Risteli M, Ruotsalainen H, Salo A, Sipilä L. Expanding the lysyl hydroxylase toolbox: new insights into the localization and activities of lysyl hydroxylase 3 (LH3). J Cell Physiol 2007;212(2):323-9.

[51] Ruotsalainen H, Sipilä L, Vapola M, Sormunen R, Salo AM, Uitto L, Mercer DK, Robins SP, Risteli M, Aszodi A, Fässler R, Myllylä R. Glycosylation catalyzed by lysyl hydroxylase 3 is essential for basement membranes. J Cell Sci 2006;119(Pt 4):625-35.

[52] Salo AM, Sipilä L, Sormunen R, Ruotsalainen H, Vainio S, Myllylä R. The lysyl hydroxylase isoforms are widely expressed during mouse embryogenesis, but obtain tissue- and cell-specific patterns in the adult. Matrix Biol 2006;25(8):475-83.

[53] Ruotsalainen H, Sipilä L, Kerkelä E, Pospiech H, Myllylä R. Characterization of cDNAs for mouse lysyl hydroxylase 1, 2 and 3, their phylogenetic analysis and tissue-specific expression in the mouse. Matrix Biol 1999;18(3):325-9.

[54] Seitzer U, Bätge B, Acil Y, Müller PK. Transforming growth factor beta 1 influences lysyl hydroxylation of collagen I and reduces steady-state levels of lysyl hydroxylase mRNA in human osteoblast-like cells. Eur J Clin Invest 1995;25(12):959-66.

[55] Knippenberg M, Helder MN, Doulabi BZ, Bank RA, Wuisman PI, Klein-Nulend J. Differential effects of bone morphogenetic protein-2 and transforming growth factor-beta1 on gene expression of collagen-modifying enzymes in human adipose tissue-derived mesenchymal stem cells. Tissue Eng Part A 2009;15(8):2213-25.

[56] van der Slot AJ, van Dura EA, de Wit EC, De Groot J, Huizinga TW, Bank RA, Zuurmond AM. Elevated formation of pyridinoline cross-links by profibrotic cytokines is associated with enhanced lysyl hydroxylase 2b levels. Biochim Biophys Acta 2005;1741(1-2):95-102.

[57] Chen JS, Mehta K. Tissue transglutaminase: an enzyme with a split personality. Int J Biochem Cell Biol 1999;31(8):817-36.

[58] Grenard P, Bates MK, Aeschlimann D. Evolution of Transglutaminase Genes: Identification of a Transglutaminase Gene Cluster on Human Chromosome 15q15. Structure of the gene encoding transglutaminase x and a novel gene family member, transglutaminase Z. J Biol Chem 2001;276(35):33066-78.

[59] Cho BR, Kim MK, Suh DH, Hahn JH, Lee BG, Choi YC, Kwon TJ, Kim SY, Kim DJ. Increased tissue transglutaminase expression in human atherosclerotic coronary arteries. Coron Artery Dis 2008;19(7):459-68.

[60] Sane DC, Kontos JL, Greenberg CS. Roles of transglutaminases in cardiac and vascular diseases. Front Biosci 2007;12:2530-45.

[61] Martinet N, Bonnard L, Regnault V, Picard E, Burke L, Siat J, Grosdidier G, Martinet Y, Vignaud JM. In vivo transglutaminase type 1 expression in normal lung, preinvasive bronchial lesions, and lung cancer. Am J Respir Cell Mol Biol 2003;28(4):428-35.

[62] Griffin M, Casadio R, Bergamini CM. Transglutaminases: nature's biological glues. Biochem J 2002;368(Pt 2):377-96.

[63] Greenberg CS, Birckbichler PJ, Rice RH. Transglutaminases: multifunctional cross-linking enzymes that stabilize tissues. FASEB J 1991;5(15):3071-7.

[64] Ta BM, Gallagher GT, Chakravarty R, Rice RH. Keratinocyte transglutaminase in human skin and oral mucosa: cytoplasmic localization and uncoupling of differentiation markers. J Cell Sci 1990;95 (Pt 4):631-8.

[65] Esposito C, Caputo I. Mammalian tranglutaminases. Identification of substrates as a key to physiological function and physiopathological relevance. FEBS J. 2005;272(3):615-31.

[66] Aeschlimann D, Thomazy V. Protein crosslinking in assembly and remodelling of extracellular matrices: the role of transglutaminases. Connect Tissue Res 2000;41(1):1-27.

[67] Griffin M, Smith LL, Wynne J. Changes in transglutaminase activity in an experimental model of pulmonary fibrosis induced by paraquat. Br J Exp Pathol 1979;60(6):653-61.

[68] Richards RJ, Masek LC, Brown RF. Biochemical and cellular mechanisms of pulmonary fibrosis. Toxicol Pathol 1991;19(4 Pt 1):526-39.

[69] Nunes I, Gleizes P-E, Metz CN, Rifkin DB. Latent transforming growth factor-β binding protein domains involved in activation and transglutaminase-dependent cross-linking of latent transforming growth factor-β. J Cell Biol 1997;136(5):1151-63.

[70] Rosenthal AK, Gohr CM, Henry LA, Le M. Participation of transglutaminase in the activation of latent transforming growth factor beta1 in aging articular cartilage. Arthritis Rheum 2000;43(8):1729-33.

[71] Vollberg TM, George MD, Nervi C, Jetten AM. Regulation of type I and type II transglutaminase in normal human bronchial epithelial and lung carcinoma cells. Am J Respir Cell Mol Biol 1992;7(1):10-8.

[72] Schittny JC, Paulsson M, Vallan C, Burri PH, Kedei N, Aeschlimann D. Protein cross-linking mediated by tissue transglutaminase correlates with the maturation of extracellular matrices during lung development. Am J Respir Cell Mol Biol 1997;17(3):334-43.

[73] Martin TR, Gerard NP, Galli SJ, Drazen JM. Pulmonary responses to bronchoconstrictor agonists in the mouse. J Appl Physiol 1988;64(6):2318-23.

[74] Roth-Kleiner M, Post M. Similarities and dissimilarities of branching and septation during lung development. Pediatr Pulmonol 2005;40(2):113-34.

[75] Bland RD, Mokres LM, Ertsey R, Jacobson BE, Jiang S, Rabinovitch M, Xu L, Shinwell ES, Zhang F, Beasley MA. Mechanical ventilation with 40% oxygen reduces pulmonary expression of genes that regulate lung development and impairs alveolar septation in newborn mice. Am J Physiol Lung Cell Mol Physiol 2007;293(5):L1099-110.

[76] Bruce MC, Bruce EN, Janiga K, Chetty A. Hyperoxic exposure of developing rat lung decreases tropoelastin mRNA levels that rebound postexposure. Am J Physiol 1993;265:L293-L300.

[77] Hudak BB, Zhang LY, Kleeberger SR. Inter-strain variation in susceptibility to hyperoxic injury of murine airways. Pharmacogenetics 1993; 3:135-143.

[78] Takaluoma K, Hyry M, Lantto J, Sormunen R, Bank RA, Kivirikko KI, Myllyharju J, Soininen R. Tissue-specific changes in the hydroxylysine content and cross-links of collagens and alterations in fibril morphology in lysyl hydroxylase 1 knock-out mice. J Biol Chem 2007 2;282(9):6588-96.

[79] van der Slot AJ, Zuurmond AM, Bardoel AF, Wijmenga C, Pruijs HE, Sillence DO, Brinckmann J, Abraham DJ, Black CM, Verzijl N, DeGroot J, Hanemaaijer R, TeKoppele JM, Huizinga TW, Bank RA. Identification of PLOD2 as telopeptide lysyl hydroxylase, an important enzyme in fibrosis. J Biol Chem 2003;278(42):40967-72.

[80] Olsen KC, Sapinoro RE, Kottmann RM, Kulkarni AA, Iismaa SE, Johnson GV, Thatcher TH, Phipps RP, Sime PJ. Transglutaminase 2 and its Role in Pulmonary Fibrosis. Am J Respir Crit Care Med 2011;184(6):699-707.

[81] Schittny JC, Paulsson M, Vallan C, Burri PH, Kedei N, Aeschlimann D. Protein Cross-linking Mediated by Tissue Transglutaminase Correlates with the Maturation of Extracellular Matrices During Lung Development. Am J Respir Cell Mol Biol 1997;17(3):334-43.

Acknowledgements

I would like to thank Prof. Dr. Werner Seeger for giving me the opportunity to carry out my thesis in his department and for providing the facilities, the equipment and the materials that were required for the experiments.

I especially wish to thank my supervisor Dr. Rory E. Morty for providing the subject of my dissertation, his constant attendance and endorsement in the laboratory, his detailed corrections of the drafts, his excellent guidance and his amicable support.

Thanks to the former and present members of the *Morty AG* at the *Max-Planck-Institute for Heart and Lung Research* for their kind assisstance, especially Simone Becker.

Last but not least I would like to thank my family, especially my brother Dr. Jens Witsch, my sister Dr. Esther Witsch and my parents Ulrike Witsch-Schöneberg and Dr. Hans-Georg Witsch for their immense support in the past.